Rainfall, Fire Risk, and Housing Prices in Hawaiʻi

Muhammad Talal Khan*[1,3], Nori Tarui[1,2], Makena Coffman[5], and Peter Fuleky[1,2,4]

[1]University of Hawaiʻi Economic Research Organization (UHERO), University of Hawaiʻi at Mānoa, Honolulu, HI, USA
[2]Department of Economics, University of Hawaiʻi at Mānoa, Honolulu, HI, USA
[3]Shidler College of Business, University of Hawaiʻi at Mānoa, Honolulu, HI, USA
[4]Corvinus Institute for Advanced Studies, Budapest, Hungary
[5]Institute for Sustainability and Resilience, University of Hawaiʻi at Mānoa, Honolulu, HI, USA

Abstract

This paper identifies the real estate market responses to rainfall and fire risk in Hawaiʻi by leveraging variations in precipitation patterns and fire risk exposure. Using transaction-level housing data between 2000 and 2019, we document three key findings. First, rainfall shocks depress property values, highlighting the disruptive impact of extreme precipitation. Second, wildfire risk also reduces property values, underscoring the market's sensitivity to fire-related hazards. Third, the negative impact of rainfall shocks is moderated in areas designated as fire zones, suggesting that buyers value the fire-mitigating benefits of increased rainfall. Our results are robust to various specifications of rainfall measures and definitions of both fire risk and fire incidence. Our findings contribute to the understanding of how compound climate risks are capitalized in real estate markets.

Keywords: Weather, Rainfall, Wildfires, Climate, Housing Markets, Hawaiʻi

JEL Classification: R10, R30, Q51, Q54

Acknowledgements

This paper is funded in part by a grant from the National Oceanic and Atmospheric Administration, Project A/AS-1-HCE-4; which is sponsored by the University of Hawaii Sea Grant College Program, SOEST, under Institutional Grant No. NA22OAR4170108 from NOAA Office of Sea Grant, Department of Commerce. The views expressed herein are those of the author(s) and do not necessarily reflect the views of NOAA or any of its subagencies.

Competing Interests

The authors have no conflicts of interest to declare.

Financial Disclosure

The authors have no relevant financial interests to disclose.

*Corresponding Author: Muhammad Talal Khan, Email: mtkhan@hawaii.edu

1 Introduction

Climate change is fundamentally altering global weather patterns, with profound implications for various sectors of the economy. Recent assessments by the Intergovernmental Panel on Climate Change (IPCC) indicate that each of the last three decades has been progressively warmer than any preceding decade since 1850, contributing to more frequent and intense extreme weather events (IPCC, 2021). In the United States, the Environmental Protection Agency reports that regions experiencing extreme single-day precipitation events have increased by approximately half a percentage point per decade between 1910 and 2020 (U.S. Environmental Protection Agency, 2021). These climatic shifts are increasingly influencing real estate decisions, as potential homebuyers express growing hesitation about purchasing properties in areas prone to climate-related risks (Redfin, 2022)

This study investigates the impact of rainfall[1] shocks on Hawai'i's real estate market, incorporating the effects of heterogeneous fire risk. Hawai'i presents a unique setting for this analysis due to its diverse microclimates resulting from the islands' steep topography and the complex interplay between terrain, trade winds, and land effects (Sen Roy and Balling, 2004; Giambelluca et al., 2013). The islands' mountains obstruct the prevailing northeast trade winds, leading to abundant precipitation on windward slopes and creating dry rain shadows in leeward areas (Figure 1).

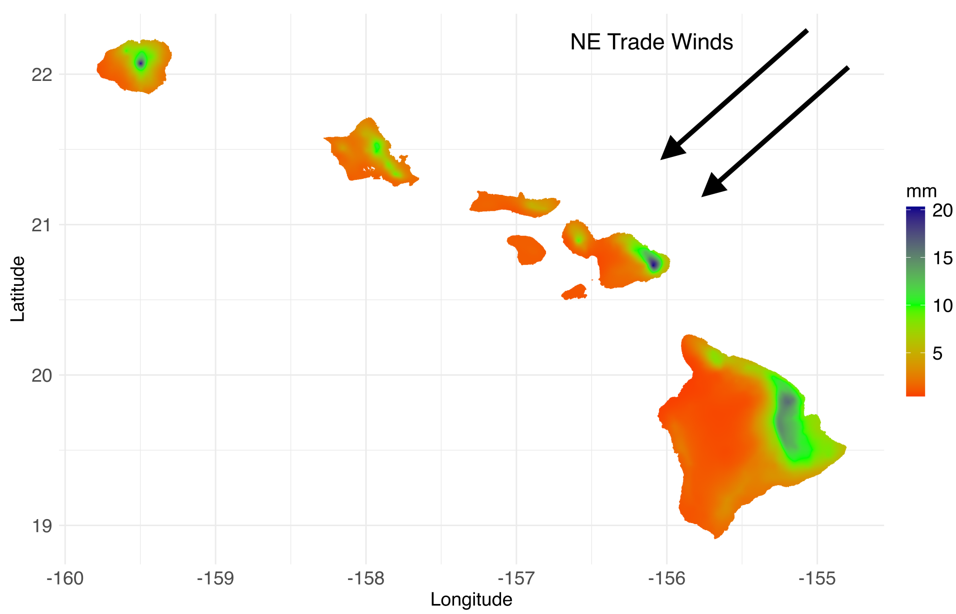

Figure 1: Average Daily Rainfall 1990-2019

Note: Rainfall in Hawai'i is concentrated on windward slopes due to the obstruction of northeast trade winds by steep topography, creating dry leeward rain shadows.

Rainfall patterns in Hawai'i have shifted in recent decades, with historically dry regions becoming drier and wet

[1] For this study *rainfall* and *precipitation* are analogous because inhabited areas in Hawai'i only experience liquid precipitation.

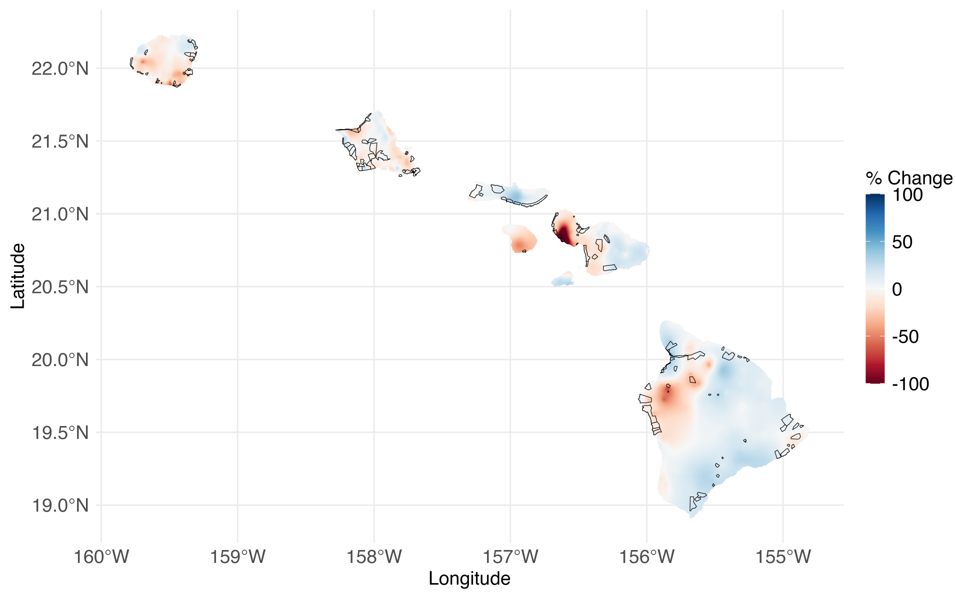

Figure 2: Percentage Change in Average Daily Rainfall: 2010–2019 vs. 1990–1999

Note: The figure shows spatial variation in rainfall trends across fire-prone areas in Hawai'i . While some excessive-risk zones have become drier, others have grown wetter, reflecting the complex interplay between precipitation and fire risk. Black polygons indicate at fire-risk communities. (Source: Hawai'i Climate Data Portal).

regions becoming wetter (Elison Timm et al., 2013; Chen and Chu, 2014). The state has also experienced more extreme precipitation events at both ends of the distribution. For example, in 2018, Kaua'i's north shore received 1,262 mm of rain in 24 hours (nearly half its annual rainfall) causing catastrophic flooding that isolated communities for months. Changes in precipitation patterns have led to increased water shortages in dry areas while amplifying risks of runoff, erosion, and flooding in wet regions (State of Hawaii Climate Change Portal, 2024).

Equally consequential is the state's growing vulnerability to wildfire. The August 2023 Lahaina wildfire underscores Hawai'i's susceptibility to destructive fires, revealing how precipitation may create countervailing effects across fire-prone zones. As Figure 2 illustrates, some areas of excessive fire risk have become wetter while others have become drier, potentially leading to mixed outcomes. Drought conditions increase the availability of combustible fuel, while excessive precipitation promotes vegetation growth that can later serve as fire fuel (Westerling et al., 2006; Lima et al., 2018; Volkova et al., 2019; Hernández Ayala et al., 2021; Puxley et al., 2024). Conversely, wet conditions can mitigate fire risk by reducing ignition probability by maintaining soil moisture (Abatzoglou and Williams, 2016), and limiting the accumulation of dry fine fuels (Van Blerk et al., 2021). This effect has been documented in tropical ecosystems (Spracklen et al., 2012) as well as in urban and forested areas (Sakai et al., 2004). Our study offers the first empirical evidence of how these nuanced precipitation-fire risk interactions are reflected in property values. The results suggest that buyers may be interpreting rainfall patterns as informative signals about local fire danger and incorporating these expectations into property valuations.

We employ two complementary estimation approaches to identify the response of consumers to rainfall variability and fire risk. First, we implement a hedonic pricing model that controls for a wide array of observable differences across properties and neighborhoods using detailed information on housing characteristics. Second, to address omitted variable bias, we estimate a repeat sales model that introduces property fixed effects. Our findings indicate that markets value the fire mitigation benefits of rainfall. Increases in rainfall consistently reduce property values; however, this negative effect is substantially moderated in areas with excessive fire risk. Specifically, a one standard deviation increase in cumulative rainfall index reduces prices by 1.9-2.1 percent in low-fire-risk areas but only 0.8 percent in excessive-risk areas. This pattern holds across multiple rainfall measures: each additional day of extreme rainfall (above the 99th percentile) reduces values by 0.7-0.8 percent in low-risk areas, but this discount is completely offset in excessive-risk areas. Extremely dry spells (below the 1st percentile) consistently reduce property values by 0.5 percent per day, regardless of fire risk exposure, while moderate dry spells have no effect. We confirm the robustness of our findings to an alternative, dynamic measure of wildfire risk that captures the proximity, size, frequency, and recency of nearby fires to reflect only salient, price-relevant risks.

The remainder of the paper is organized as follows. Section 2 reviews the relevant literature. Section 3 describes the data sources, our fire risk measures, and their construction. Section 5 motivates our empirical strategy by documenting the increasing importance of environmental risks in Hawaiʻi . Section 4 details the construction of our precipitation measures. Section 6 outlines the empirical approach. Section 7 presents the main findings, and Section 8 discusses their implications and proposes directions for future research.

2 Literature Review

A growing body of research documents how climate risks are increasingly capitalized into real estate values. Recent work has established that markets discount properties exposed to sea level rise (SLR) nationally, with the magnitude varying based on local adaptation capacity and risk awareness (Fu et al., 2016; Bernstein et al., 2019; Keys and Mulder, 2020; Tedesco et al., 2020; Tarui et al., 2023; Tyndall, 2023). Similar pricing patterns have been observed for other climate hazards. Wildfires have been linked to increased mortgage delinquency (Issler et al., 2020) and reduced residential property values (Dong, 2024), hurricanes, and extreme heat to declines in commercial real estate returns (Addoum et al., 2024; Cvijanovic and Van de Minne, 2024). This extensive body of work highlights the responsiveness of real estate markets to climate risks. However, since environmental amenities exhibit heterogeneous effects across local conditions (Gibbons et al., 2014; Albouy et al., 2016; Bakkensen and Barrage, 2021), the channels and magnitudes of these market responses remain subjects of ongoing debate.

Rainfall poses a distinctive case because it functions both as an amenity and a disamenity. Early hedonic studies found a negative impact of rainfall on property values (Blomquist et al., 1988; Clark and Cosgrove, 1990). Torrential rainfall and flooding risk are associated with lower housing prices (Bin and Landry, 2013) and tighter lending standards (Avril et al., 2023; Blickle et al., 2024). In general, households prefer less precipitation and more seasonal variation (Englin, 1996).

Recent work reveals important nuances in the relationship between precipitation property value. Goodwin et al. (2021) shows that increased rainfall in Mexico City reduces particulate matter pollution, indirectly boosting home prices through improved air quality. Mueller et al. (2018) document how post-wildfire flooding risks in Arizona create compound effects on property values, highlighting the interplay between different climate hazards. Lamas Rodríguez et al. (2023)

finds a negative correlation between ecological deterioration caused by excessive rainfall and house prices in Mar Menor, Spain. Choi and Lee (2016) look at the physical amount of rainfall as one cause of floods and find that both the average annual rainfall and rain intensity (amount of rainfall per rainy day) negatively affect property prices. Overall, this strand of literature suggests that the impact of rainfall on property values is negative but may vary based on its interaction with other environmental factors.

Ecological research provides important context for these interactions. Drought conditions increase fuel dryness and ignition potential, whereas periods of heavy precipitation promotes vegetation growth that subsequently serves as combustible fuel (Westerling et al., 2006; Holden et al., 2018; Lima et al., 2018; Volkova et al., 2019; Hernández Ayala et al., 2021; Puxley et al., 2024). Conversely, ignition probability and fuel flammability may also be strongly moderated by recent precipitation and moisture conditions (Abatzoglou and Williams, 2016; Van Blerk et al., 2021). The dual role of precipitation in both amplifying and mitigating fire risk highlights the need to understand how the Hawaiian housing market interprets these opposing ecological signals.

Beyond physical exposure, housing markets reflect how agents form and update beliefs about environmental risks. Empirical work shows that property prices respond more to salient or recent events than to objective hazard probabilities. Following natural disasters, capitalization effects spike but gradually dissipate as memory fades (Hallstrom and Smith, 2005; Bin and Landry, 2013; Gallagher, 2014; McCoy and Walsh, 2018). These patterns align with experience-based learning frameworks, wherein buyers update perceived risk after observing new signals (Baldauf et al., 2020; Boustan et al., 2020; Bakkensen and Barrage, 2021). In this view, rainfall anomalies may act as informational signals that alter beliefs about future fire hazard realization, i.e., increased rain in excessive fire-risk areas may signal reduced ignition risk to potential buyers.

We test this expectation-based mechanism in the Hawaiian housing market. Hawai'i provides an ideal setting for this analysis due to its diverse microclimates and varying exposure to fire risk. Following Englin's (1996) caution against national-level precipitation studies, we focus on a region where spatially granular rainfall measurement is available and fire risk varies substantially in small geographic areas. We construct z-score-based indices, which have been widely used in climate impact studies due to their simplicity and reliability in assessing climate vulnerability (Shahabfar et al., 2012; Nam and Kim, 2013; Nourani et al., 2021; Pauline et al., 2021; Zaveri et al., 2023). We also consider a suite of alternative measures, such as fractional deviation of monthly rainfall from its average historical level (Duflo and Pande, 2007; Sarsons, 2015), rainfall shocks (Jayachandran, 2006; Sarsons, 2015; Shah and Steinberg, 2017; Kaur, 2019), and counts of extreme rainy and dry days, identified by a percentile threshold (Suppiah and Hennessy, 1998; Endo et al., 2005; Méndez-Lázaro et al., 2014).

We employ two measures of fire exposure to distinguish between long-term structural vulnerability and short-term environmental salience. The static Communities at Risk (CAR) classification, established in 2006–2007, captures baseline hazard potential determined by persistent landscape characteristics such as vegetation density, topography, and historical fire incidence. These features define a property's inherent susceptibility to wildfire but remain constant over time. Our second measure, following Shi et al. (2022), is a dynamic fire exposure index that incorporates the size, proximity, and recency of actual wildfire events within a defined spatial and temporal window. This index accounts for evidence that hazard-related price effects are strongest following salient events (Hallstrom and Smith, 2005; Bin and Landry, 2013). Note that if rainfall merely corrected for a mismeasured or outdated fire risk classification, its interaction with the fire measure would disappear once the dynamic index reflecting contemporary weather conditions is used. Instead, consistent results across both measures would indicate that rainfall conveys distinct, time-varying information about ignition probability. In this framework, rainfall functions as an environmental signal that markets use to update expectations about immediate fire danger.

Methodologically, our work contributes to a debate about the appropriate empirical strategies for identifying climate-related price effects. The traditional hedonic approach (Rosen, 1974) has been widely used to estimate implicit prices of environmental amenities but faces challenges from omitted variables. To address this, first, we include a host of controls in our regression, including basic property characteristics (square footage, rooms, property age, home type, slope etc.), coastal proximity controls as properties close to the coast command a premium (Jin et al., 2015; Tarui et al., 2023), and elevation controls as high elevation is viewed as an amenity due to superior views (Gordon et al., 2013), or as insurance against risks such as SLR (Tyndall, 2023). Second, we utilize a repeat sales method to address omitted variable concerns (Palmquist, 2005). Our implementation of both approaches demonstrates how they can provide complementary evidence on environment-property value relationships.

This paper advances understanding of how compound climate risks shape real estate values. We provide new evidence on the interaction between precipitation patterns and fire risk in determining property values. Our methodological framework, combining hedonic and repeat-sales approaches, can be extended to other contexts where multiple environmental processes jointly affect asset values.

3 Data

3.1 Parcel Data

This study employs real estate transaction data and key property characteristics from Black Knight, a financial services firm. Our analysis is underpinned by property assessment and deed data. The deed data provides critical transactional information, including the exact date of the transaction and the classification of the property as either residential or commercial. The assessment data offers insights into property features such as the number of rooms, living area, age of the property, and type (e.g., single-family dwelling vs. multi-family dwelling). These two datasets are merged using the Black Knight Distinct Property ID (BKDPID), a unique identifier for each property. Our study focuses exclusively on residential properties. We used transactions between 2000 and 2019 and excluded transactions priced below $50,000 or above $50,000,000 to retain arm's length transactions and remove outlier influence.

In the subsequent phase, we integrated environmental data, starting with publicly accessible daily rainfall rasters from the Hawai'i Climate Data Portal. This product is gridded at a high resolution of 250 meters, allowing us to use it effectively with detailed micro-transaction data. In addition, we procured GIS shapefiles from the Hawai'i Statewide GIS Program's Geospatial Data Portal, which offered detailed spatial geometries of tax parcels and delineations of coastlines across the principal Hawaiian islands. These rainfall rasters were overlaid onto our parcel geometries to generate a spatial map. The projection chosen for this analytical exercise was the WGS-1984, deemed most suitable for our geographic study area. For each day from January 1, 1990, through December 31, 2019, we assigned to each parcel the daily precipitation value as its value at the parcel's geographical center. This procedure was then replicated with additional shapefiles, augmenting the dataset with other critical spatial attributes such as elevation and coastal distance. We mapped elevation rasters onto

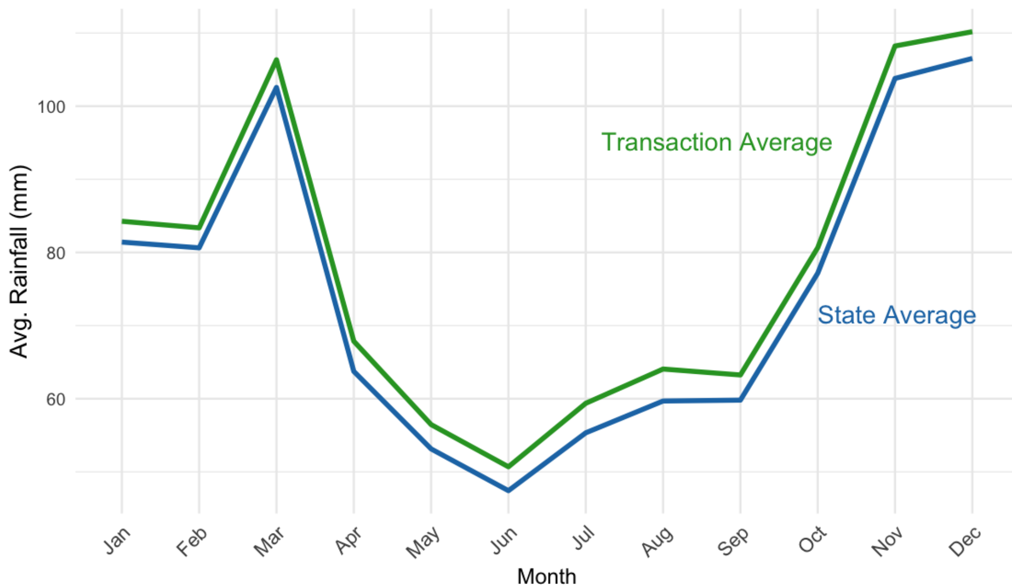

Figure 3: Average Monthly Rainfall (mm) from 1990 to 2019

Note: This figure shows average monthly rainfall from 1990–2019, comparing the state-level average (blue) with the average for transactions in our sample (green). Monthly values represent the mean rainfall per property, averaged across 30 years.

parcels to calculate the average gradient of the parcel (slope). Utilizing Assessor Parcel Number (APN) as the property identifier, we merged this augmented dataset with Black Knight data.

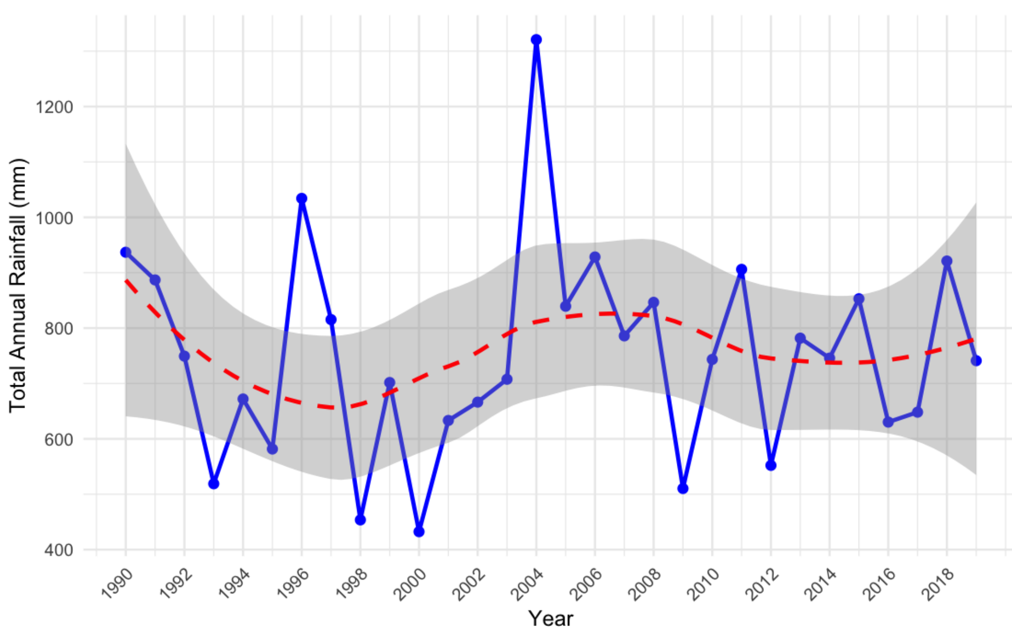

Figure 4: Total Annual Rainfall (mm)

Note: This figure plots the total annual rainfall for properties in our transaction sample. The solid blue line connects yearly totals, while the dashed red line shows a smoothed LOESS trend to highlight long-run patterns in precipitation.

Figure 3 illustrates average monthly rainfall patterns for the state and for properties in our sample from 1990–2019. While the sample properties exhibit higher average rainfall overall, the pattern closely aligns with statewide seasonal fluctuations. Rainfall in Hawaiʻi is characterized by distinct wet (November–March) and dry (April–October) seasons. During the wet season, trade winds bring precipitation primarily to windward areas, supplemented by winter storms that can produce rainfall across the islands. In the dry season, precipitation declines significantly, especially in leeward regions, although windward areas continue to receive some rainfall driven by trade winds. The long-term trend in total annual rainfall remained relatively stable from 1990 to 2019 (Figure 4, dashed red line).

3.2 Static Fire Risk

We obtain fire risk data from the Hawaiʻi Statewide GIS Program's Communities at Risk (CAR) from the Wildland Fires layer. Initially compiled in 2006-2007 by the Department of Land and Natural Resources, this dataset provides risk ratings of High, Medium, or Low for major populated areas across the Hawaiian islands. The fire risk assessment follows guidelines developed by the National Association of State Foresters in June 2003, created in response to the National Fire Plan and the Healthy Forests Restoration Act (HFRA). These guidelines outline a process for identifying and prioritizing communities at risk from wildland fires, considering factors such as fire occurrence, hazard conditions, values protected, and protection capabilities. In our analysis, we designate a community at risk of "excessive fire" if rated as either high or medium risk.[2] Despite the data being collected in 2006-2007, the Hawaiʻi Statewide GIS Program confirmed in October 2022 that these boundaries and risk ratings remain valid and unchanged over time.

3.3 Dynamic Fire Risk

Although, the static classification reflects underlying landscape vulnerability, it may not fully capture evolving on-the-ground conditions. Figure A5 shows that actual wildfire perimeters often diverge from the mapped risk boundaries. To complement the static designation, we therefore construct a dynamic transaction-specific fire index that accounts for recent wildfire activity surrounding each property. This index integrates the size, proximity, and frequency of wildfires occurring within three years and 10km of each sale, similar to Shi et al. (2022):

$$\text{FireIndex}_{it} = \sum_k \frac{\text{size}_{kt}^{\alpha}}{\exp(\text{distance}_{kt})}, \tag{1}$$

where size_{kt} is the area of fire k (acres) and distance_{kt} is its centroid distance (km) from property i. The exponential term introduces spatial decay, and α allows for diminishing marginal effects of fire size. Wildfire perimeters are compiled from the Pacific Fire Exchange database, which merges ground-mapped, satellite, and agency sources including the Hawaiʻi Wildfire Management Organization, US Geological Survey, and the University of Hawaiʻi Department of Natural Resources and Environmental Management.

The time-varying measure of fire exposure, constructed from actual wildfire occurrences, serves as a validation check for our baseline results. It mitigates potential measurement concerns associated with the static risk map and captures capitalization effects driven by the salience of recent fires (Bin and Landry, 2013; McCoy and Walsh, 2018). Details of the index construction and the estimation of α are provided in Appendix A. For clarity and interpretability, we rely on the

[2] While we group high and medium fire risk areas to reflect broader exposure, the results are robust to separating these categories. Both show consistent patterns compared to low-risk areas, and the main findings remain unchanged.

Table 1: Summary Statistics (2000-2019)

	Mean	Median	Sd	Min.	Max.
Panel A: Full Sample					
Sales Price	495,513	356,773	698,757	50,000	46,117,500
Fire Risk	0.59	1	0.49	0	1
House Age	26	26	18	0	166
Square Footage (1000)	1.4	1.1	0.82	0.1	21
# Bedrooms	2.7	3	1.2	1	18
Slope	3.6	2.3	4	0	47
Elevation (m)	98	25	172	0	1584
Coastal Distance (m)	2,659	1,456	3,347	0.47	25,108
Single Family	0.41	0	0.49	0	1
Six Month Daily Avg (mm)	2.6	1.9	2.4	0.02	35
Panel B: Repeat Sales Sample					
Sales Price	474,870	345,000	644,470	50000	46,117,500
Fire Risk	0.62	1.00	0.49	0	1.00
House Age	25	25	17	0	166
Square Footage (1000s)	1.3	1.1	0.80	0.1	17
# Bedrooms	2.6	3	1.2	1	15
Slope	3.6	2.3	4	0	42
Elevation (m)	97	24	171	0	1469
Coastal Distance (m)	2,632	1,410	3,334	0.47	24,614
Single Family	0.4	0	0.49	0	1
Six Month Daily Avg (mm)	2.57	1.85	2.33	0.02	35.14

Note: Descriptive statistics for all transactions. Fire Risk is a binary indicator. Zero house age indicates the property was sold the same year it was built. All prices are nominal. N = 268,406 for the full sample and N = 180,044 for the repeat sales sample.

static designation as our primary measure of wildfire risk and report the dynamic index results as a robustness exercise in the appendix.

3.4 Summary Statistics

Our final dataset consists of 268,406 observations covering 158,405 unique properties in the four counties of Maui, Kauaʻi , Honolulu, and Hawaiʻi . Restricting this to properties that sold more than once, 33% of observations drop out. Table 1 provides descriptive statistics for the full sample and repeat sales subsample, highlighting key property characteristics and differences across the datasets. The nominal median sales price for the full sample was $356,773, while the repeat sales subsample had a slightly lower median of $345,000. Properties in the full sample were, on average, 26 years old, with a mean size of 1,400 square feet. The average six-month daily rainfall was 2.6 mm across both samples. In the full sample, 59 percent of transactions occurred in communities classified as at excessive fire risk under the static designation. Under the dynamic measure, 43 percent of transactions exhibited some wildfire exposure within the prior three years of transaction date. The mean fire index of 0.41 and median of 0 indicate that most properties faced minimal exposure, while the maximum value of 18 points to a small number of transactions located near large or repeated fires (Table A4).

Table 2 further disaggregates the full sample by fire risk, illustrating notable differences. Properties in excessive-fire-

Table 2: Comprehensive Sample Summary Statistics split by Fire Risk (2000-2019)

	Low Fire Risk					**Excessive Fire Risk**				
	Mean	**Median**	**Std. dev.**	**Min.**	**Max.**	**Mean**	**Median**	**Std. dev.**	**Min.**	**Max.**
Sales Price	505,352	365,000	724,534	50,000	46,117,500	488,610	350,000	680,005	50,000	41,775,000
House Age	31	31	18	0	162	22	21	16	0	166
Square Footage (1000)	1.3	1.1	0.87	0	21	1.4	1.2	0.79	0	14
# Bedrooms	2.5	2	1.3	1	18	2.7	3	1.1	1	16
Slope	3.4	1.9	4.2	0	42	3.8	2.6	3.9	0	47
Elevation (m)	101	18	201	0	1,584	95	30	148	0	1,401
Coastal Distance (m)	2,652	1,486	3,629	0.49	25,108	2,663	1,439	3,134	0.47	22,887
Single Family	0.38	0	0.49	0	1	0.42	0	0.49	0	1
Six Month Daily Avg (mm)	3.2	2.2	2.8	0.031	35	2.2	1.7	1.9	0.016	16

Note: Descriptive statistics for all transactions categorized by excessive fire risk (N = 110,676) and low fire risk (N = 157,730). All prices are nominal.

risk areas were generally newer (mean age of 22 years) and larger (1,400 square feet on average) compared to low-fire-risk areas (mean age of 31 years, 1,300 square feet). Average six-month daily rainfall was higher in low fire-risk areas (3.2 mm) than in high fire-risk areas (2.2 mm). These differences underscore the geographic and environmental variation in the dataset, enabling an in-depth analysis of rainfall impacts on property values across fire risk profiles.

Figure 5 shows the distribution of sales prices which has a rightward skew. In our regression specifications, we use logarithm-transformed nominal sales price as our dependent variable, which approximately follows a normal distribution. Our repeat sales sample is also representative of the complete set of home sales (Figure A1).

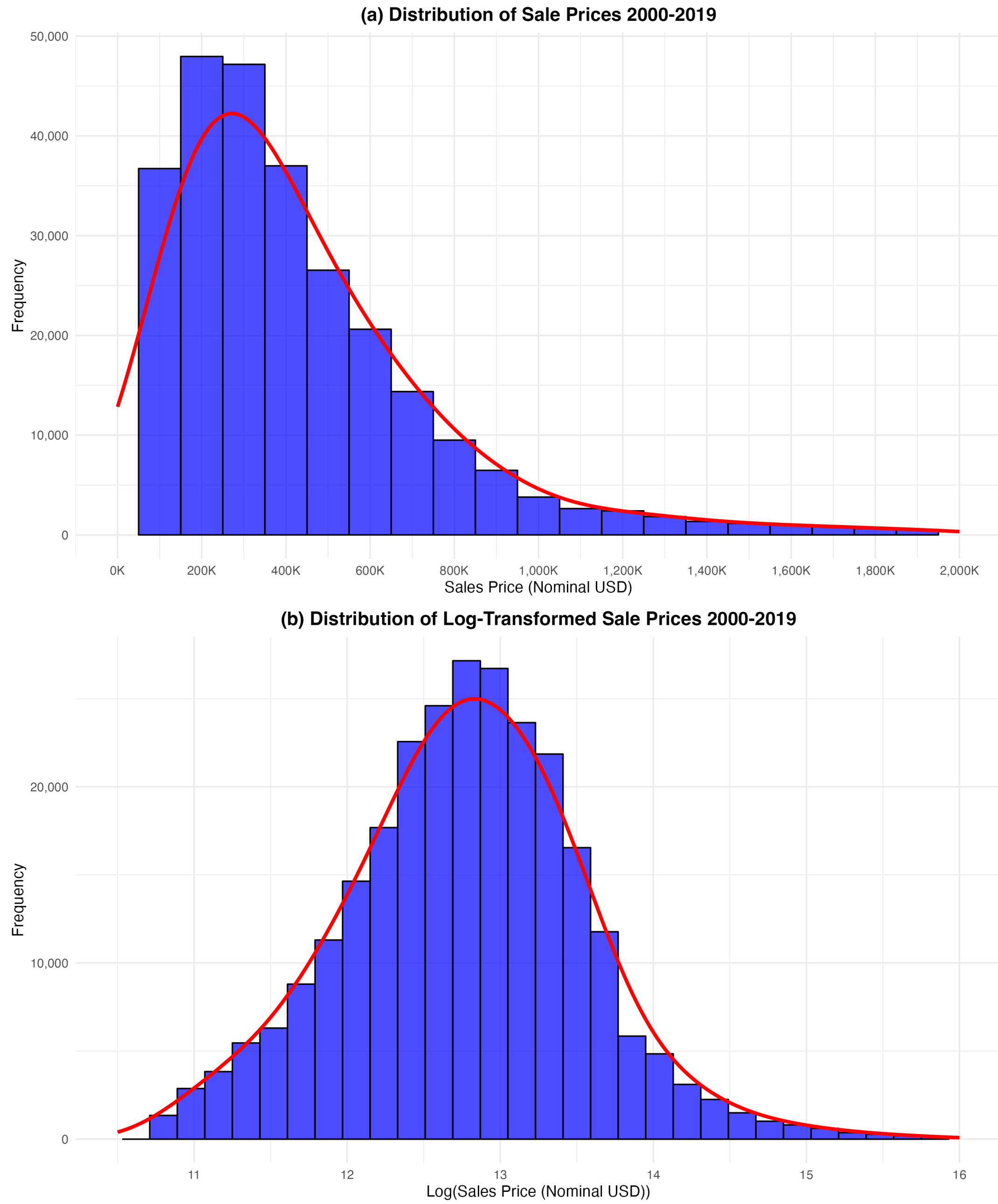

Figure 5: Nominal Sales Price Distributions 2000-2019

4 Precipitation Measures

To quantify the relationship between precipitation patterns and property prices, we utilize various indices: Cumulative Rain Index (CRI), Fractional Deviation (FD), Shock Index (SI), Rain Event Count (REC), and Dry Event Count (DEC). Each index is computed for individual property transactions. For notational simplicity, we suppress the time subscript throughout our discussion of these indices, although each measure is calculated specifically for a property's transaction date.

4.1 Cumulative Rain Index (CRI)

Z-score-based indices, or standardized precipitation anomalies, are widely used in the literature to quantify precipitation variability (Zaveri et al., 2023). Typically, these involve subtracting location-specific rainfall from its long-term mean and dividing by the standard deviation across the entire sample. Rainfall variability measured in this manner reflects random draws from the climate distribution (Zaveri et al., 2023). The resulting z-score represents the standard deviations from the long-run mean for a specific location and time. Our Cumulative Rain Index (CRI) extends this concept with some modifications. We define lookback periods (90, 180, or 365 days) before each property's transaction date. We compare this lookback period with a mean for the same calendar days during the prior 10 years, controlling for both location-specific and seasonal factors.

Calculating the long-term mean based on 10 years of daily observational data preceding our lookback period offers several advantages. First, it captures recent weather trends, as the baseline adjusts with each property's transaction date, allowing the index to adapt to evolving precipitation patterns potentially influenced by climate change. Second, according to Gourley (2021), recent weather conditions have a more statistically significant impact on house prices than long-term averages. Third, the approach flexibly adjusts for the volatility of weather, i.e. whether a property is in a region with a stable climate or one experiencing rapid changes, the index will reflect the relevant recent conditions relative to the norm. Our index is calculated as follows:

- For each property i, we consider N days (N = 90, 180, 365) of daily rainfall data immediately preceding the transaction date. This is our lookback period.
- For property i with transaction date t, we identify the same N calendar days in each year during the ten-year base period preceding the lookback period. For example, assuming $N = 180$ and the property sold on January 1, 2010, the lookback period would be July 5, 2009, to January 1, 2010 (180 days). The base period would cover July 5 to January 1 for each year from 1999 to 2008. This approach ensures consistency in seasonality between the lookback and base periods.
- The CRI for property i is the difference between the cumulative rainfall in the lookback period R_{lookback_i} and the mean of the cumulative rainfalls in each year of the base period μ_{base_i}, scaled by the standard deviation of the cumulative rainfall per year in the base period $\sigma^*_{\text{base}_i}$. Note that the base period means and standard deviations are computed from ten cumulative rainfall observations (one for each year in the base period).

$$\text{CRI}_i = \frac{R_{\text{lookback}_i} - \mu_{\text{base}_i}}{\sigma_{\text{base}_i}} \tag{2}$$

For robustness, we also analyze the index constructed using a fixed 1990-1999 base period to examine the impact of long-term climate change rather than short-term weather variations.

4.2 Fractional Deviation (FD)

We use a commonly used measure of rainfall shocks constructed to account for seasonality, i.e., the fractional deviation of monthly rainfall from its average level (Duflo and Pande, 2007; Sarsons, 2015). The average is calculated for each month using data from 1990 to 1999. This fixed base period allows FD to account for long-term shifts in rainfall patterns, making it a potential proxy for climate change over the years. We define a shock for each of the 12 months preceding the transaction date and sum them to obtain the overall rainfall shock for each property. Specifically:

- For property i in month m, calculate the historical average across $BaseYears = \{1990, 1991, \ldots, 1999\}$. This gives us twelve average values for January through December.

$$\bar{R}_{i,m} = \frac{1}{10} \sum_{y \in \text{BaseYears}} R_{i,m,y} \tag{3}$$

- For each of the twelve months m preceding the transaction, calculate the fractional deviation from the historical average of that month.

$$\delta_{i,m} = \frac{R_{i,m} - \bar{R}_{i,m}}{\bar{R}_{i,m}} \tag{4}$$

- Sum the deviations for each of the 12 months preceding the transaction date and divide by twelve to compute the average fractional deviation for property i:

$$\text{FD}_i = \frac{1}{12} \sum_{m=1}^{12} \delta_{i,m} \tag{5}$$

4.3 Shock Index (SI)

We construct a seasonally adjusted measure of rainfall shocks based on the approach used in Jayachandran (2006), Sarsons (2015), and Kaur (2019).

- For each property i and each month m (January through December), we compute the 80th and 20th percentile total rainfall values, denoted as $P80_{i,m}$ and $P20_{i,m}$, respectively. These percentiles are computed using total rainfall data across the $BaseYears = \{1990, 1991, \ldots, 1999\}$, providing ten data points for each month.
- For each of the twelve months preceding the transaction month, we look at the total monthly rainfall $R_{i,m}$ and define a discrete shock $S_{i,m}$ to represent a positive, negative, or no shock.

$$S_{i,m} = \begin{cases} +1, & \text{if } R_{i,m} > P80_{i,m} \\ -1, & \text{if } R_{i,m} < P20_{i,m} \\ 0, & \text{if } P20_{i,m} \leq R_{i,m} \leq P80_{i,m} \end{cases} \tag{6}$$

- Calculate the average of the monthly shocks over the twelve months preceding the transaction date to obtain the rainfall shock measure for property i:

$$\text{Shock}_i = \frac{1}{12} \sum_{m=1}^{12} S_{i,m} \tag{7}$$

4.4 Rain Event Count (REC) and Dry Event Count (DEC)

To capture the frequency of unusual rainfall events and their potential impact on property prices, we employ metrics called Rain Event Count (REC) and Dry Event Count (DEC). These measures are designed to quantify how often precipitation deviates significantly from historical norms, providing a measure of extreme weather occurrences. REC focuses on unusually wet periods, calculated at the 90th, 95th, and 99th percentiles of historical rainfall. Conversely, DEC captures unusually dry periods, focusing on the 1st, 5th, and 10th percentiles. By examining both extremes, we aim to provide a comprehensive picture of precipitation anomalies that could influence property valuations. This approach allows us to capture not just the intensity but also the frequency of extreme weather events, which may have non-linear effects on property markets. The indices are calculated as follows:

- For each property transaction, we consider 365 days (12 months) of daily rainfall data immediately preceding the transaction date. This is our lookback period.
- For the same property, we use historical data over the past 10 years to calculate the respective percentile thresholds.
- For REC we count the number of days in the lookback period that exceed these thresholds.
- For DEC we count the number of days in the lookback period that are below these thresholds.

4.5 Precipitation Summary Statistics

Panel A of Table 3 presents summary statistics for our rainfall measures, revealing substantial variations in precipitation patterns across our comprehensive sample. These measures are designed to capture different aspects of rainfall shocks, from cumulative deviations to extreme events. The Cumulative Rain Index (CRI_{365}), which measures the standardized deviation of rainfall over a 365-day lookback period, shows a mean of 0.13 and a median of 0.07. This slight positive skew, coupled with a standard deviation of 1.30 and a range from -5.62 to 6.66, indicates that while on average, properties experienced slightly wetter conditions than historical norms, there was considerable variability, with some areas experiencing significantly drier and others wetter conditions. The Fractional Deviation (FD) measure captures the average cumulative rainfall anomalies over the 12 months preceding each property transaction. With a mean of 0.1 and a median of 0.01, it suggests that, on average, properties experienced slightly higher cumulative rainfall in the year leading up to the transaction compared to their historical norms. Specifically, the mean indicates that over the year leading up to the transaction, properties experienced a consistent pattern of increased rainfall, averaging 10% more than what is typically expected based on historical data. The median of 0.01 implies that half of the observations had an average fractional deviation within 1% of their historical average during the prior 12 months. The standard deviation of 0.43 and the wide range from -0.85 to 3.24 highlight significant variability in rainfall patterns across different properties and periods. In extreme cases, some areas experienced only 25% of their normal cumulative rainfall (severe drought conditions), while others received more than three times their typical amount (extreme excess rainfall) in the year preceding a transaction.

The Shock Index (SI), which discretizes monthly rainfall into positive, negative, or no shocks based on historical 80th and 20th percentiles, provides additional insight into the frequency and direction of rainfall anomalies. With a mean of 0.05 and a median of 0.00, it suggests a slight tendency towards positive rainfall shocks in our sample period. The full range of -1.00 to 1.00 indicates that some properties experienced consistently dry or consistently wet conditions relative to their historical norms over the 12 months preceding the transaction.

We measure extreme rainfall frequency using Rain Event Counts (REC) above the 90th, 95th, and 99th percentiles over a 365-day period. On average, properties have 39.40 days (median 39) above the 90th percentile, 20.64 days (median 20) above the 95th, and 4.47 days (median 4) above the 99th, closely matching theoretical expectations of 37, 18, and 4 days, respectively. Maximum values of 119, 64, and 29 days, respectively, reflect substantial variation across transactions. Dry Event Counts (DEC) are lower: 33.5 days (median 36) below the 10th percentile and 0.40 days (median 0) below the 1st percentile. Notably, properties experience more than eleven times as many days above the 99th percentile than below the 1st, indicating a skew toward wet extremes.

Table 3: Rainfall Measure Summary Statistics

	Mean	Median	Sd	Min	Max
Panel A: Full Sample					
CRI_{365}	0.13	0.07	1.30	-5.62	6.66
FD	0.09	0.01	0.43	-0.85	3.24
SI	0.05	0.01	0.49	-1.00	1.00
$REC_{>90\%}$	39.40	39.00	13.09	4.00	119.00
$REC_{>95\%}$	20.64	20.00	8.62	0.00	64.00
$REC_{>99\%}$	4.47	4.00	3.21	0.00	29.00
$DEC_{<10\%}$	33.48	36.00	20.32	0.00	124.00
$DEC_{<5\%}$	13.50	14.00	12.57	0.00	83.00
$DEC_{<1\%}$	0.40	0.00	1.69	0.00	23.00
Panel B: Repeat Sales Sample					
CRI_{365}	0.15	0.09	1.31	-5.41	6.66
FD	0.10	0.01	0.44	-0.85	3.24
SI	0.06	0.01	0.49	-1.00	1.00
$REC_{>90\%}$	39.59	39.00	13.18	4.00	119.00
$REC_{>95\%}$	20.76	20.00	8.69	0.00	64.00
$REC_{>99\%}$	4.49	4.00	3.26	0.00	29.00
$DEC_{<10\%}$	32.87	36.00	20.42	0.00	123.00
$DEC_{<5\%}$	13.21	13.00	12.50	0.00	69.00
$DEC_{<1\%}$	0.38	0.00	1.61	0.00	22.00

Note: Rainfall measure descriptive statistics based on all transactions (N = 268,406) and repeat sales transactions (N = 180,044). The Cumulative Rain Index (CRI) is calculated over a lookback period of 365 days before the transaction date, reflecting cumulative rainfall deviations. Fractional Deviation (FD) captures rainfall shocks using monthly deviations from a historical average for each of the 12 months preceding the transaction date. The Shock Index (SI) is based on discrete monthly rainfall shocks, where rainfall in each of the 12 months deviates beyond the 80th or below the 20th percentiles of historical values. Rain Event Count (REC) and Dry Event Count (DEC) quantify extreme daily events, counting the number of days exceeding or falling below-specified rainfall percentiles within the 365-day lookback period.

Panel B demonstrates similar patterns, indicating consistency in rainfall measures across the repeat sales subsample. Overall, the variability in precipitation patterns, from sustained shifts in average rainfall to fluctuations in extreme wet and dry events, offers a robust foundation for analyzing the impact of changing rainfall regimes on property values across Hawaiʻi's diverse micro-climates.

5 Saliency

Do homebuyers in Hawaiʻi internalize the state's micro-climatic variations when making purchase decisions? Evidence from both rainfall and wildfire patterns suggests that these environmental risks are becoming increasingly difficult to ignore. Figure 6 shows that properties in our sample have experienced a growing number of days with extreme rainfall.[3] Five-year moving averages suggest that this shift represents a structural change in precipitation patterns rather than isolated weather events, particularly evident in the mid-2000s when extreme rainfall often exceeded its full-sample mean. Likewise, wildfire risk has also intensified. Approximately 0.5% of Hawaiʻi's total land area burns annually, a rate comparable to or even exceeding that of any other US state. Figure 7 illustrates the trend in statewide area burned over time.

In Appendix A, we present additional evidence that microclimate distinctions are recognizable concerns in Hawaiʻi

[3]We follow the common practice in climate studies of using 75mm as a cutoff for extreme rainfall. This rule of thumb threshold has been adopted in regional studies (Beguería and Vicente-Serrano, 2006) and appears in Hawaiʻi's climate assessments and academic work (Chu et al., 2009; Kunkel et al., 2022).

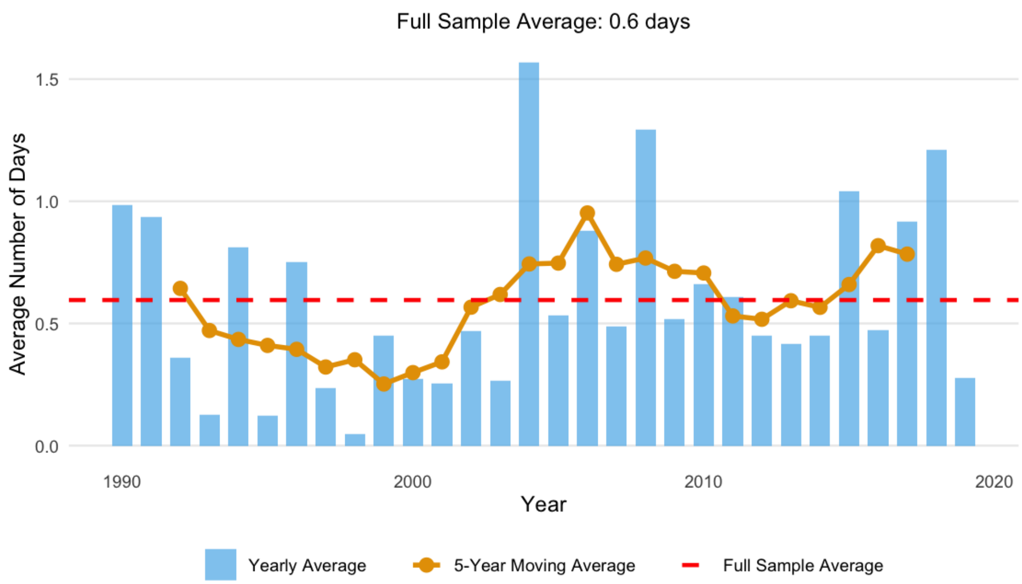

Figure 6: Average Extreme Precipitation Days by Property

Note: This figure tracks each unique property in our sample and reports the average number of days with extreme rainfall (over 75 mm) between 1990–2019. The increase in both frequency and clustering after the mid-2000s suggests a structural shift in precipitation patterns across the sample period.

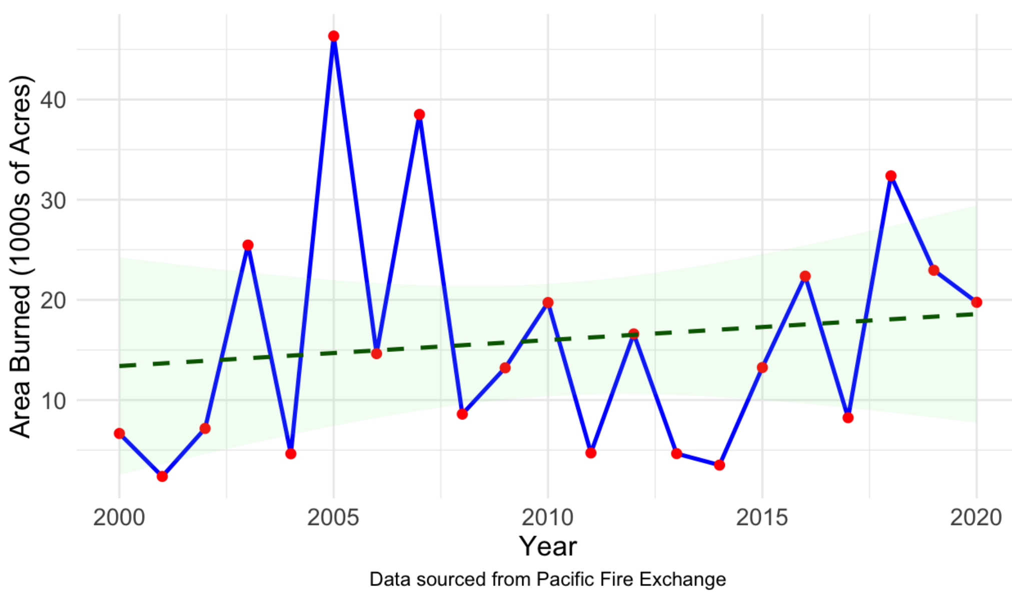

Figure 7: Annual Area Burned Statewide

Note: This figure shows the area (in thousands of acres) burned by wildfires in Hawai'i from 2000 to 2020, with a fitted linear trend line and 95% confidence interval. Data is sourced from the Pacific Fire Exchange.

, particularly the "windward" versus "leeward" dichotomy. These terms frequently appear in real estate listings and search patterns. Public disclosure of localized environmental risk can shift buyer behavior. For example, Donovan et al.

(2007) found that after the Colorado Springs Fire Department's risk ratings became publicly accessible, properties in high-risk areas saw their previous amenity premiums offset by increased risk awareness among buyers. In Hawai'i , websites like the Rainfall Atlas of Hawai'i and the Pacific Fire Exchange have been accessible since 2011, providing spatial data on precipitation trends and wildfire incidents. Hawai'i buyers have thus long had access to the data necessary to make informed location decisions based on environmental risks.

A key empirical challenge concerns the horizon over which buyers process and respond to environmental risks. To address this, we complement our analysis with a dynamic fire index that incorporates the size, proximity, frequency, and recency of fires (Appendix A). Our approach thus accounts for the salience-driven capitalization documented in the natural disaster literature, where risk is reflected in home prices primarily after major events (Bin and Landry, 2013; McCoy and Walsh, 2018). Similarly, our rainfall measures discussed in Section 4 are designed to align with short time frames over which environmental conditions are most likely to influence property valuations.

6 Methods

We use a hedonic regression to examine the heterogeneous impact of rainfall on property values between 2000-2019 across areas with different levels of fire risk.[4] Our estimating Equation 8 controls for housing characteristics to isolate the effect of precipitation changes:

$$\log(P_{it}) = \beta_1 W_{it} + \beta_2 F_i + \beta_3 (W_{it} \cdot F_i) + X_{it}\gamma_x + Y_t + C_i + \epsilon_{it} \tag{8}$$

The variable P_{it} represents the log-price of property i in transaction year t, W_{it} is a placeholder for our wetness measure, F_i is a binary variable that is one if fire risk is excessive, the vector X_{it} represents the property characteristics including property type (Single Family vs Multi Family), house age, living area square footage, total rooms, number of bedrooms, slope of the property, and 20 equal sized control bins for elevation and coastal proximity. Year-month fixed effects Y capture market-wide fluctuations in home prices over time, and census tract fixed effects C absorb time-invariant neighborhood characteristics. Consequently, our identification stems from within census tract variation in our wetness measure. The coefficient β_1 captures the average effect of changes in precipitation on log property prices in areas with low fire risk ($F_i = 0$), holding all other factors constant. For excessive fire risk areas ($F_i = 1$), the β_2 coefficient represents the price premium or discount associated with high fire risk regardless of precipitation levels, and the β_3 coefficient shows how the effect of precipitation on property prices differs in excessive fire risk areas compared to low fire risk areas. We interpret the rainfall–fire interaction as capturing how rainfall shocks modify the salience of risk within structurally exposed zones. The total effect of precipitation on log property prices in excessive fire risk areas is given by $\beta_1 + \beta_3$.

To account for the possibility of unobserved differences in housing characteristics, we also estimate a repeat sales model given in Equation 9. The repeat sales approach isolates the average difference in log price experienced by a specific property due to changes in precipitation levels between sales, while also accounting for how this effect varies with fire risk. Identification now stems from variations in precipitation through time across repeat sales.

[4] We experimented with alternative functional forms, including Box-Cox transformations and non-linear (e.g., squared) terms for house age and size, but found minimal differences in estimates. As most omitted variable bias concerns are addressed using the repeat sales approach, we do not report model fit statistics (e.g., AIC, BIC, R^2) for these variants.

$$\log(P_{it}) = \beta_1 W_{it} + \beta_2(W_{it} \cdot F_i) + \beta_3(F_i \cdot T_i) + \beta_4(C_i \cdot T_i) + Y_t + H_i + \epsilon_{it} \quad (9)$$

Property fixed effects H_i control for all time-invariant characteristics of the property, including those that are observable (such as location, elevation, or basic structural features) and those that are unobservable, mitigating the concerns for omitted variable bias. The year-month fixed effects Y_t continue to control for market-wide temporal variation and the interpretation of β_1 and β_2 remains the same: heterogeneous impact of precipitation in high and and low fire risk areas. Note that we do not control directly for F_i, as being in high vs low risk is absorbed by the property fixed effects. We do control for the possibility that properties may appreciate differently in excessive fire risk areas by including $(F_i \cdot T_i)$, where T_i is a continuous year variable generated from the transaction date (i.e., a property sold at the end of the sixth month of 2012 would take the value of 2012.5). The coefficient β_3 captures the yearly difference in price appreciation between excessive and low fire risk properties. Similarly, the term $(C_i \cdot T_i)$ captures the time trend in property appreciation by census tract which accounts for how preferences for different census tracts may have changed over time.

For both hedonic and repeat sales specifications, we apply a two-way clustering adjustment to standard errors since ϵ_{it} may be correlated across space and time. The effect of precipitation on properties in the same neighborhood is likely similar, which justifies clustering at the census tract level. Temporally, we cluster at the year-month level to account for the correlation of precipitation patterns within months.

7 Results

Our hedonic model provides insights into how various property characteristics and rainfall patterns influence housing prices in Hawai'i , with a particular focus on areas with different levels of fire risk (Table 4). The control coefficients in our hedonic model align with conventional expectations in the real estate literature. We find that living area is positively associated with property values, with each additional 1,000 square feet corresponding to a 25% higher price ($p<0.01$). This substantial effect underscores the premium placed on spacious homes in Hawai'i's market. Similarly, each additional bedroom is associated with a 3% price gain ($p<0.01$), reflecting the value of functional living space. Single-family homes command a significant premium of 20% ($p<0.01$) over multi-family dwellings. The positive coefficient for average slope (0.5% per unit increase, $p<0.01$) suggests that properties on steeper terrain are more valuable. Conversely, house age has a small negative effect (-0.4% per additional year, $p<0.01$), indicating a preference for newer properties. Irrespective of precipitation, properties in excessive-fire-risk areas sell at about an 8-15% discount.

Turning to variables of primary interest, we find that higher precipitation levels, as proxied by various measures, negatively affect property values in low-fire-risk areas. The Cumulative Rain Index (CRI_{365}) coefficient indicates that a one unit higher index, representing one standard deviation higher rainfall at a particular location, is associated with 1.9% lower property values ($p < 0.01$) in low fire risk areas. However, the effect differs markedly in excessive-fire-risk areas, where the same increase corresponds to only a 0.8% decrease in property values. Additional measures, including the Fractional Deviation (FD), Shock Index (SI), and Rain Event Count (REC), provide further insights. A one-unit increase in FD is associated with a 6% decline in property values ($p < 0.01$) in low-fire-risk areas. This negative impact is fully reversed in excessive-fire-risk areas, where a mild positive effect of 0.6% is observed. Similarly, a one-unit increase in SI corresponds to a 2.4% decline in property values ($p < 0.05$) in low-fire-risk areas, while excessive-fire-risk areas exhibit 1.8% higher property values.

Table 4: Hedonic Regression Results

	Dependent Variable: Log(Sales Price)						
	CRI_{365}	FD	SI	$REC_{>90}$	$REC_{>99}$	$DEC_{<10}$	$DEC_{<1}$
Index	-0.019***	-0.061***	-0.024**	-0.003***	-0.008***	0.000	-0.005***
	(0.003)	(0.013)	(0.011)	(0.000)	(0.001)	(0.000)	(0.001)
Index × Fire Risk	0.011***	0.067***	0.042***	0.002***	0.010***	-0.001***	0.000
	(0.002)	(0.011)	(0.009)	(0.000)	(0.001)	(0.000)	(0.002)
Fire Risk	-0.083**	-0.086**	-0.084**	-0.148***	-0.124***	-0.082**	-0.082**
	(0.038)	(0.038)	(0.038)	(0.039)	(0.038)	(0.038)	(0.038)
House Age	-0.004***	-0.004***	-0.004***	-0.004***	-0.004***	-0.003***	-0.004***
	(0.000)	(0.000)	(0.000)	(0.000)	(0.000)	(0.000)	(0.000)
Living Area (1000 sq. ft.)	0.252***	0.252***	0.252***	0.252***	0.252***	0.252***	0.252***
	(0.006)	(0.006)	(0.006)	(0.006)	(0.006)	(0.006)	(0.006)
Bedrooms	0.030***	0.030***	0.030***	0.030***	0.030***	0.030***	0.030***
	(0.003)	(0.003)	(0.003)	(0.003)	(0.003)	(0.003)	(0.003)
SFR	0.202***	0.201***	0.202***	0.202***	0.201***	0.202***	0.202***
	(0.009)	(0.009)	(0.009)	(0.009)	(0.009)	(0.009)	(0.009)
Avg. Slope	0.005***	0.005***	0.005***	0.005***	0.005***	0.005***	0.005***
	(0.001)	(0.001)	(0.001)	(0.001)	(0.001)	(0.001)	(0.001)
Num. Obs.	268,406	268,406	268,406	268,406	268,406	268,406	268,406
R^2	0.728	0.728	0.728	0.728	0.728	0.728	0.728
Adj. R^2	0.716	0.716	0.716	0.716	0.716	0.716	0.716
Census FE	Y	Y	Y	Y	Y	Y	Y
Year-month FE	Y	Y	Y	Y	Y	Y	Y

Note: Significance levels: *** p<0.01, ** p<0.05, * p<0.1. Two-way clustered standard errors in parentheses. This table presents hedonic regression results corresponding to Equation 8. CRI_{365} (Cumulative Rainfall Index, 365-day), FD (Fractional Deviation), SI (Shock Index), REC (Rain Event Count), and DEC (Dry Event Count) are different measures of precipitation patterns. Subscripts for REC and DEC indicate percentile thresholds, with both measures calculated based on a 365-day lookback period. All models include twenty equal sized control bins for elevation and coastal proximity.

In low fire risk areas, each additional day of rainfall above the 90th percentile ($REC_{>90}$) is associated with a 0.3% lower property value (p<0.01), while a day above the 99th percentile ($REC_{>99}$) corresponds to a 0.8% lower value (p<0.01). In excessive fire risk areas, the coefficients are 0.1% and 0.2%, respectively. The Dry Event Count (DEC) measures show that dry days must be very extreme to negatively impact property values. An additional day below the 10th percentile ($DEC < 10$) has no impact on property values, but an additional day below the 1st percentile ($DEC < 1$) of rainfall is associated with a 0.5% decrease in property values ($p < 0.01$) in both excessive and low fire risk areas. Notably, the effect of dry conditions does not show a significant interaction with fire risk, unlike the wet conditions captured by REC. This suggests that the relationship between precipitation patterns and fire risk may not be reciprocal: increased wetness reduces fire risk, but increased dryness does not proportionally increase it, at least as perceived by the housing market.

Our repeat sales model corroborates the hedonic model findings while addressing potential omitted variable bias through its control of time-invariant property characteristics (Table 5). The coefficients for rainfall indices remain notably consistent between both models. For instance, a one standard deviation increase in CRI corresponds to a 2.1% decrease in property values (p<0.05) in low fire risk areas, closely matching the 1.9% effect observed in the hedonic model. Similarly,

Table 5: Repeat Sales Regression Results

	Dependent Variable: Log(Sales Price)						
	CRI_{365}	FD	SI	$REC_{>90}$	$REC_{>99}$	$DEC_{<10}$	$DEC_{<1}$
Index	-0.021***	-0.057***	-0.019	-0.003***	-0.007***	0.000	-0.005**
	(0.003)	(0.017)	(0.012)	(0.000)	(0.002)	(0.000)	(0.002)
Index × Fire Risk	0.013***	0.078***	0.052***	0.002***	0.010***	-0.001**	-0.004
	(0.003)	(0.014)	(0.012)	(0.000)	(0.001)	(0.000)	(0.003)
Fire Risk × Year	-0.005***	-0.004***	-0.005***	-0.005***	-0.004***	-0.005***	-0.005***
	(0.002)	(0.001)	(0.002)	(0.002)	(0.001)	(0.002)	(0.002)
Num. Obs.	180,044	180,044	180,044	180,044	180,044	180,044	180,044
R^2	0.880	0.881	0.880	0.881	0.881	0.880	0.880
Adj. R^2	0.804	0.804	0.804	0.804	0.804	0.804	0.804
Property FE	Y	Y	Y	Y	Y	Y	Y
Year-month FE	Y	Y	Y	Y	Y	Y	Y
Census Time Trend	Y	Y	Y	Y	Y	Y	Y

Note: Significance levels: *** $p<0.01$, ** $p<0.05$, * $p<0.1$. Two-way clustered standard errors in parentheses. This table presents repeat sales regression results corresponding to Equation 9. CRI_{365} (Cumulative Rainfall Index, 365-day), FD (Fractional Deviation), SI (Shock Index), REC (Rain Event Count), and DEC (Dry Event Count) are different measures of precipitation patterns. Subscripts for REC and DEC indicate percentile thresholds, with both measures calculated based on a 365-day lookback period.

the fire risk-mitigating benefits of rainfall persist with properties in excessive-risk areas showing only a 0.8% depreciation following precipitation. Properties in fire risk areas face an annual price appreciation penalty of 0.5%, indicating an accumulating long-term cost to being in these risk zones.

Collectively, our findings in the hedonic and repeat sales model indicate that while rainfall generally decreases property values, this negative effect is substantially moderated in fire-prone areas. The divergence suggests that housing markets capitalize the protective function of rainfall against fire hazards in vulnerable areas.

8 Discussion and Conclusion

The relationship between precipitation and fire risk operates through multiple channels that may have countervailing effects on property values. Drought conditions enhance fire risk by increasing the availability of combustible fuel (Westerling et al., 2006; Lima et al., 2018; Puxley et al., 2024). Conversely, periods of excessive precipitation can promote vegetation growth that subsequently becomes potential fire fuel under dry conditions (Volkova et al., 2019; Hernández Ayala et al., 2021). However, wet conditions may also reduce fire risk through several mechanisms: maintaining higher soil moisture that reduces ignition probability (Abatzoglou and Williams, 2016), limiting the accumulation of dry fine fuels (Van Blerk et al., 2021), and altering vegetation moisture content. These mitigating effects have been documented across diverse ecosystems, from tropical regions (Spracklen et al., 2012) to urban-wildland interfaces (Sakai et al., 2004).

Our results show that rainfall generally exerts a negative effect on property values, reflecting its nuisance and flood potential. However, this effect is substantially moderated in fire-prone areas, suggesting that buyers interpret rainfall as a signal of reduced ignition risk and incorporate these expectations into property valuations. The attenuation is robust across rainfall metrics, regression specifications, and alternative definitions of fire exposure. Such market behavior parallels documented responses to other natural hazards where risk perceptions drive price dynamics (Hallstrom and Smith, 2005;

Bin and Landry, 2013).

The magnitude of these effects is economically significant. While a one unit higher cumulative rainfall index (which is equivalent to a one standard deviation increase in precipitation) corresponds to 1.9% lower property values in low-fire-risk areas, this negative effect shrinks to 0.8% in high-risk areas. This difference suggests that markets assign substantial value to the role of precipitation in fire risk mitigation. Similarly, each additional day of extreme rainfall (above the 99th percentile) is associated with 0.8% lower home values in low fire-risk areas but this effect reverses to 0.2% higher home value in excessive-risk areas.

Three implications follow. First, there is value in further exploring whether real estate markets process compound climate risks correctly. While our results show that buyers respond to precipitation–fire risk linkages, these responses occur amid evolving ecological and scientific understanding (Westerling et al., 2006; Abatzoglou and Williams, 2016). As precipitation patterns grow more volatile, improved public communication and disclosure could help align market perceptions with physical realities.

Second, the heterogeneous impact of rainfall across fire-risk zones underscores the need for spatially differentiated adaptation strategies. Although markets already adjust to varying levels of exposure, the increasing frequency of compound climate events may warrant complementary policy interventions. Local governments could strengthen land-use planning, building codes, and vegetation management in excessive-risk zones to enhance resilience alongside market-based adjustments.

Third, our results inform ongoing debates about climate adaptation in spatially granular contexts. Hawai'i's diverse microclimates and varying exposure to fire risk create valuable variation for studying climate-property value relationships. The substantial price discounts we document in fire risk areas (8-15%) suggest a significant market valuation of fire risk, with potential implications for public investment in risk mitigation infrastructure extending beyond Hawai'i's unique context.

Several promising directions for future research emerge from our analysis. While we document how markets process climate risks in Hawai'i's setting, investigating whether similar patterns exist in other regions would illuminate the broader applicability of our findings. Studies could examine how variations in risk communication affect market pricing of compound climate risks. Future work should also consider moral hazard implications. If rainfall makes excessive-risk areas appear safer, it may inadvertently attract more development, complicating adaptation efforts. Unfortunately, such analysis is currently precluded in Hawai'i due to restrictive zoning and data constraints.

In conclusion, our findings reveal that markets actively price both precipitation and fire risks through measurable effects on property values. The observed price patterns suggest that buyers weigh precipitation's role in fire risk when valuing properties, contributing to a growing literature on how real estate markets price compound climate risks. As communities worldwide confront intersecting environmental hazards, understanding these market responses becomes increasingly relevant for policy design.

References

Abatzoglou, J. T. and Williams, A. P. (2016). Impact of anthropogenic climate change on wildfire across western US forests. *Proceedings of the National Academy of Sciences*, 113(42):11770–11775.

Addoum, J. M., Eichholtz, P., Steiner, E., and Yönder, E. (2024). Climate change and commercial real estate: Evidence from Hurricane Sandy. *Real Estate Economics*, 52(3):687–713.

Albouy, D., Ehrlich, G., and Liu, Y. (2016). Housing demand, cost-of-living inequality, and the affordability crisis. NBER Working Paper 22816, National Bureau of Economic Research.

Avril, P., Levieuge, G., and Turcu, C. (2023). Typhoons in China: Do bankers want their umbrellas back when it rains? *SSRN Electronic Journal*.

Bakkensen, L. A. and Barrage, L. (2021). Going underwater? Flood risk belief heterogeneity and coastal home price dynamics. *The Review of Financial Studies*, 35(8):3666–3709.

Baldauf, M., Garlappi, L., and Yannelis, C. (2020). Does climate change affect real estate prices? Only if you believe in it. *The Review of Financial Studies*, 33(3):1256–1295.

Beguería, S. and Vicente-Serrano, S. M. (2006). Mapping the hazard of extreme rainfall by peaks over threshold extreme value analysis and spatial regression techniques. *Journal of Applied Meteorology and Climatology*, 45(1):108–124.

Bernstein, A., Gustafson, M. T., and Lewis, R. (2019). Disaster on the horizon: The price effect of sea level rise. *Journal of Financial Economics*, 134(2):253–272.

Bin, O. and Landry, C. E. (2013). Changes in implicit flood risk premiums: Empirical evidence from the housing market. *Journal of Environmental Economics and Management*, 65(3):361–376.

Blickle, K., Perry, E., and Santos, J. A. (2024). Do mortgage lenders respond to flood risk? Staff Report 1101, Federal Reserve Bank of New York.

Blomquist, G. C., Berger, M. C., and Hoehn, J. P. (1988). New estimates of quality of life in urban areas. *The American Economic Review*, 78(1):89–107.

Boustan, L. P., Kahn, M. E., Rhode, P. W., and Yanguas, M. L. (2020). The effect of natural disasters on economic activity in US counties: A century of data. *Journal of Urban Economics*, 118:103257.

Case, B. and Quigley, J. M. (1991). The dynamics of real estate prices. *The Review of Economics and Statistics*, 73(1):50–58.

Chen, Y. R. and Chu, P.-S. (2014). Trends in precipitation extremes and return levels in the Hawaiian Islands under a changing climate. *International Journal of Climatology*.

Choi, M. and Lee, J. (2016). Hedonic valuation of flood. *WIT Transactions on Ecology and the Environment*, 204:187–195.

Chu, P.-S., Zhao, X., Ruan, Y., and Grubbs, M. (2009). Extreme rainfall events in the Hawaiian Islands. *Journal of Applied Meteorology and Climatology*, 48(3):502–516.

Clapp, J. M., Giaccotto, C., and Tirtiroglu, D. (1991). Housing price indices based on all transactions compared to repeat subsamples. *Real Estate Economics*, 19(3):270–285.

Clark, D. E. and Cosgrove, J. C. (1990). Hedonic prices, identification, and the demand for public safety. *Journal of Regional Science*, 30(1):105–121.

Conley, T. G. (1999). GMM estimation with cross sectional dependence. *Journal of econometrics*, 92(1):1–45.

Cvijanovic, D. and Van de Minne, A. (2024). Temperature extremes and commercial real estate. *Available at SSRN 4517557*.

Dong, H. (2024). Climate change and real estate markets: An empirical study of the impacts of wildfires on home values in California. *Landscape and Urban Planning*, 247:105062.

Donovan, G. H., Champ, P. A., and Butry, D. T. (2007). Wildfire risk and housing prices: A case study from Colorado Springs. *Land Economics*, 83(2):217–233.

Duflo, E. and Pande, R. (2007). Dams. *The Quarterly Journal of Economics*, 122(2):601–646.

Dufour, J.-M. and Neves, J. (2019). Chapter 1 - Finite-sample inference and nonstandard asymptotics with Monte Carlo tests and R. In *Conceptual Econometrics Using R*, volume 41 of *Handbook of Statistics*, pages 3–31. Elsevier.

Elison Timm, O., Takahashi, M., Giambelluca, T. W., and Diaz, H. F. (2013). On the relation between large-scale circulation pattern and heavy rain events over the Hawaiian Islands: Recent trends and future changes. *Journal of Geophysical Research: Atmospheres*, 118(10):4129–4141.

Endo, N., Ailikun, B., and Yasunari, T. (2005). Trends in precipitation amounts and the number of rainy days and heavy rainfall events during summer in China from 1961 to 2000. *Journal of the Meteorological Society of Japan. Ser. II*, 83(4):621–631.

Englin, J. (1996). Estimating the amenity value of rainfall. *The Annals of Regional Science*, 30:273–283.

Fu, X., Song, J., Sun, B., and Peng, Z.-R. (2016). "Living on the edge": Estimating the economic cost of sea level rise on coastal real estate in the Tampa Bay region, Florida. *Ocean & Coastal Management*, 133:11–17.

Gallagher, J. (2014). Learning about an infrequent event: Evidence from flood insurance take-up in the United States. *American Economic Journal: Applied Economics*, pages 206–233.

Gatzlaff, D. H. and Haurin, D. R. (1997). Sample selection bias and repeat-sales index estimates. *The Journal of Real Estate Finance and Economics*, 14:33–50.

Giambelluca, T. W., Chen, Q., Frazier, A. G., Price, J. P., Chen, Y.-L., Chu, P.-S., Eischeid, J. K., and Delparte, D. M. (2013). Online rainfall atlas of Hawai 'i. *Bulletin of the American Meteorological Society*.

Gibbons, S., Mourato, S., and Resende, G. M. (2014). The amenity value of English nature: A hedonic price approach. *Environmental and Resource Economics*, 57:175–196.

Goodwin, M. B., Fontenla, M., and Gonzalez, F. (2021). Estimating the impact of pollution on wages and housing prices using satellite imagery. *Applied Economics Letters*, 28(20):1750–1753.

Gopalakrishnan, S. and Klaiber, H. A. (2014). Is the shale energy boom a bust for nearby residents? Evidence from housing values in Pennsylvania. *American Journal of Agricultural Economics*, 96(1):43–66.

Gordon, B., Winkler, D., Barrett, D., and Zumpano, L. (2013). The effect of elevation and corner location on oceanfront condominium value. *Journal of Real Estate Research*, 35(3):345–364.

Gourley, P. (2021). Curb appeal: How temporary weather patterns affect house prices. *The Annals of Regional Science*, 67(1):107–129.

Hallstrom, D. G. and Smith, V. K. (2005). Market responses to hurricanes. *Journal of Environmental Economics and Management*, 50(3):541–561.

Hansen, W. D. and Naughton, H. T. (2013). The effects of a spruce bark beetle outbreak and wildfires on property values in the wildland–urban interface of south-central Alaska, USA. *Ecological Economics*, 96:141–154.

Hernández Ayala, J. J., Mann, J., and Grosvenor, E. (2021). Antecedent rainfall, excessive vegetation growth and its relation to wildfire burned areas in California. *Earth and Space Science*, 8(9):e2020EA001624.

Holden, Z. A., Swanson, A., Luce, C. H., Jolly, W. M., Maneta, M., Oyler, J. W., Warren, D. A., Parsons, R., and Affleck, D. (2018). Decreasing fire season precipitation increased recent western US forest wildfire activity. *Proceedings of the National Academy of Sciences*, 115(36):E8349–E8357.

Holmes, T. P., Prestemon, J. P., and Abt, K. L. (2008). *The economics of forest disturbances: Wildfires, storms, and invasive species*, volume 79. Springer Science & Business Media.

IPCC (2021). *Climate Change 2021: The Physical Science Basis. Contribution of Working Group I to the Sixth Assessment Report of the Intergovernmental Panel on Climate Change*, volume In Press. Cambridge University Press, Cambridge, United Kingdom and New York, NY, USA.

Issler, P., Stanton, R., Vergara-Alert, C., and Wallace, N. (2020). Mortgage markets with climate-change risk: Evidence from wildfires in California. *Available at SSRN 3511843*.

Jayachandran, S. (2006). Selling labor low: Wage responses to productivity shocks in developing countries. *Journal of Political Economy*, 114(3):538–575.

Jin, D., Hoagland, P., Au, D. K., and Qiu, J. (2015). Shoreline change, seawalls, and coastal property values. *Ocean & Coastal Management*, 114:185–193.

Kaur, S. (2019). Nominal wage rigidity in village labor markets. *American Economic Review*, 109(10):3585–3616.

Keys, B. J. and Mulder, P. (2020). Neglected no more: Housing markets, mortgage lending, and sea level rise. Technical report, National Bureau of Economic Research.

Kunkel, K., Frankson, R., Runkle, J., Champion, S., Stevens, L., Easterling, D. R., Stewart, B., McCarrick, A., and Lemery, C. (2022). State Climate Summaries for the United States 2022. NOAA Technical Report NESDIS 150. Technical report, NOAA NESDIS.

Lamas Rodríguez, M., Garcia Lorenzo, M. L., Medina Magro, M., and Perez Quiros, G. (2023). Impact of climate risk materialization and ecological deterioration on house prices in Mar Menor, Spain. *Scientific Reports*, 13(1):11772.

Lima, C. H., AghaKouchak, A., and Randerson, J. T. (2018). Unraveling the role of temperature and rainfall on active fires in the Brazilian Amazon using a nonlinear Poisson model. *Journal of Geophysical Research: Biogeosciences*, 123(1):117–128.

Loomis, J. (2004). Do nearby forest fires cause a reduction in residential property values? *Journal of forest economics*, 10(3):149–157.

McCluskey, J. J. and Rausser, G. C. (2001). Estimation of perceived risk and its effect on property values. *Land Economics*, 77(1):42–55.

McCoy, S. J. and Walsh, R. P. (2018). Wildfire risk, salience & housing demand. *Journal of Environmental Economics and Management*, 91:203–228.

Méndez-Lázaro, P. A., Nieves-Santiango, A., and Miranda-Bermúdez, J. (2014). Trends in total rainfall, heavy rain events, and number of dry days in San Juan, Puerto Rico, 1955-2009. *Ecology and Society*, 19(2).

Mueller, J., Loomis, J., and González-Cabán, A. (2009). Do repeated wildfires change homebuyers' demand for homes in high-risk areas? A hedonic analysis of the short and long-term effects of repeated wildfires on house prices in Southern California. *The Journal of Real Estate Finance and Economics*, 38:155–172.

Mueller, J. M., Lima, R. E., Springer, A. E., and Schiefer, E. (2018). Using matching methods to estimate impacts of wildfire and postwildfire flooding on house prices. *Water Resources Research*, 54(9):6189–6201.

Nam, K.-P. and Kim, C.-H. (2013). Study on sensitivity of different standardization methods to climate change vulnerability index. *Journal of Environmental Impact Assessment*, 22(6):677–693.

Nourani, V., Najafi, H., Sharghi, E., and Roushangar, K. (2021). Application of Z-numbers to monitor drought using large-scale oceanic-atmospheric parameters. *Journal of Hydrology*, 598:126198.

OECD, Eurostat, International Monetary Fund, and World Bank (2013). *Handbook on residential property price indices*. Eurostat, Luxembourg.

Palmquist, R. B. (2005). Property value models. *Handbook of Environmental Economics*, 2:763–819.

Pauline, E. L., Knox, J. A., Seymour, L., and Grundstein, A. J. (2021). Revising NCEI's climate extremes index and the CDC's social vulnerability index to analyze climate extremes vulnerability across the United States. *Bulletin of the American Meteorological Society*, 102(1):E84–E98.

Puxley, B. L., Martin, E., Basara, J., and Christian, J. I. (2024). The wildfire impacts of the 2017-2018 precipitation whiplash event across the Southern Great Plains. *Environmental Research Letters*, 19(7):074029.

Ready, R. C. and Abdalla, C. W. (2005). The amenity and disamenity impacts of agriculture: Estimates from a hedonic pricing model. *American Journal of Agricultural Economics*, 87(2):314–326.

Redfin (2022). 62% of homebuyers, sellers hesitant to move to area with climate risk. Accessed on November 16, 2024.

Rosen, S. (1974). Hedonic prices and implicit markets: Product differentiation in pure competition. *Journal of Political Economy*.

Sakai, A., Hagihara, Y., Asada, K., and Shengping, Z. (2004). Management of rainfall-related environmental risks in urban area. *Journal of Risk Research*, 7(7-8):731–744.

Sarsons, H. (2015). Rainfall and conflict: A cautionary tale. *Journal of Development Economics*, 115:62–72.

Sen Roy, S. and Balling, R. C. (2004). Analysis of Hawaiian diurnal rainfall patterns. *Theoretical and Applied Climatology*, 79(3):209–214.

Shah, M. and Steinberg, B. M. (2017). Drought of opportunities: Contemporaneous and long-term impacts of rainfall shocks on human capital. *Journal of Political Economy*, 125(2):527–561.

Shahabfar, A., Ghulam, A., and Eitzinger, J. (2012). Drought monitoring in Iran using the perpendicular drought indices. *International Journal of Applied Earth Observation and Geoinformation*, 18:119–127.

Shi, L., Chen, B., Chen, X., and Chen, Z. (2022). Assessing the impact of wildfires on property values in wildland-urban intermix and interface in Colorado: A hedonic approach. *Journal of Environmental Management*, 319:115672.

Spracklen, D. V., Arnold, S. R., and Taylor, C. (2012). Observations of increased tropical rainfall preceded by air passage over forests. *Nature*, 489(7415):282–285.

State of Hawaii Climate Change Portal (2024). Less and heavy rain. Accessed on November 16, 2024.

Stetler, K. M. (2008). Capitalization of environmental amenities and wildfire in private home values of the wildland–urban interface of northwest Montana, USA. Master's thesis, The University of Montana, College of Forestry and Conservation, Missoula, MT. Unpublished master's thesis, 175 pp.

Stetler, K. M., Venn, T. J., and Calkin, D. E. (2010). The effects of wildfire and environmental amenities on property values in northwest Montana, USA. *Ecological Economics*, 69(11):2233–2243.

Suppiah, R. and Hennessy, K. J. (1998). Trends in total rainfall, heavy rain events and number of dry days in Australia, 1910-1990. *International Journal of Climatology: A Journal of the Royal Meteorological Society*, 18(10):1141–1164.

Tarui, N., Urbanski, S., Lam, Q. L., Coffman, M., and Newfield, C. (2023). Sea level rise risk interactions with coastal property values: A case study of O 'ahu, Hawai 'i. *Climatic Change*, 176(9):130.

Tedesco, M., McAlpine, S., and Porter, J. R. (2020). Exposure of real estate properties to the 2018 Hurricane Florence flooding. *Natural Hazards and Earth System Sciences*, 20(3):907–920.

Tyndall, J. (2023). Sea level rise and home prices: Evidence from Long Island. *The Journal of Real Estate Finance and Economics*, 67(4):579–605.

U.S. Environmental Protection Agency (2021). Climate change indicators: Heavy precipitation. Accessed on November 16, 2024.

Van Blerk, J., West, A., Altwegg, R., and Hoffman, M. (2021). Post-fire summer rainfall differentially affects reseeder and resprouter population recovery in fire-prone shrublands of South Africa. *Science of the Total Environment*, 788:147699.

Volkova, L., Weiss Aparicio, A. G., and Weston, C. J. (2019). Fire intensity effects on post-fire fuel recovery in Eucalyptus open forests of south-eastern Australia. *Science of The Total Environment*, 670:328–336.

Westerling, A. L., Hidalgo, H. G., Cayan, D. R., and Swetnam, T. W. (2006). Warming and earlier spring increase western US forest wildfire activity. *Science*, 313(5789):940–943.

Xu, Z. and Van Kooten, G. C. (2013). Living with wildfire: The impact of historic fires on property values in Kelowna, BC. Working Paper 2013-05, Resource Economics and Policy Analysis Research Group, Department of Economics, University of Victoria.

Zaveri, E. D., Damania, R., and Engle, N. L. (2023). Droughts and deficits: The global impact of droughts on economic growth. Policy Research Working Paper Series 10453, The World Bank.

A Appendix

A.1 Repeat Sales Framework

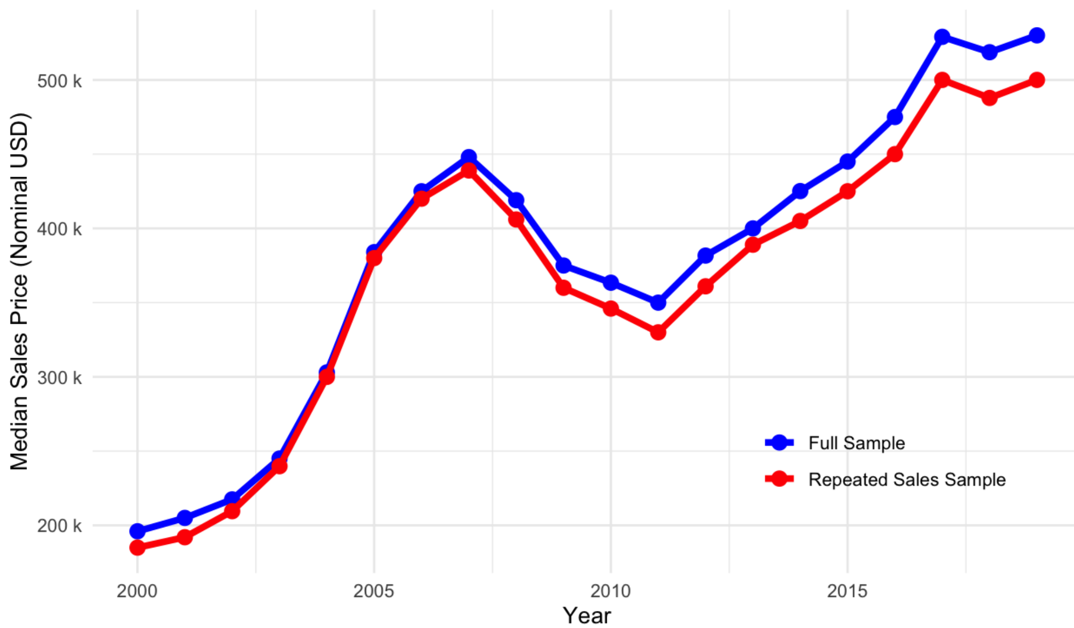

Figure A1: State Level Trend in Median Sales Price by Sample Type

Figure A1 shows that median home prices in Hawaiʻi have continued to appreciate since 2000, reaching a high in 2007, right around the time of the global financial crisis. They then depreciated until 2011 but have since been appreciating steadily, reaching new highs near the end of our sample. Importantly, Figure A1 also plots the median sales price trend of the repeated sales sub-sample, which only includes properties that sold more than once. While repeat sales address the issue of unobserved differences in housing characteristics, the method may be less precise than hedonic models due to smaller sample sizes and potential selection bias issues (Gatzlaff and Haurin, 1997; OECD et al., 2013; Case and Quigley, 1991). However, if the quality of homes is similar, arbitrage will force prices for the repeat sample to grow at the same rate as the prices for the full sample (Clapp et al., 1991), which is what we observe in Figure A1. The trends of the repeated sales and the full sample of sales are very closely related, with a correlation coefficient of 0.99. Conducting a Kolmogorov–Smirnov (KS) test on the density of log sales price of the repeat sale and full sample, we fail to reject the null hypothesis that there is no difference between the two distributions ($D = 0.05$, $p = 0.69$)[5]. Overall, the repeat sales sample is representative of the broader real estate market.

To further probe the validity of the repeat sales approach, we restrict the sample to properties that transacted exactly twice. If repeat sales bias is driven by transaction frequency, as suggested by Tyndall (2023), then this restriction should yield estimates that better reflect underlying market trends. Next, we exclude properties with holding periods less than four years to mitigate potential distortion from speculative behavior. Results for these are consistent with our main

[5]The K-S test compares the empirical distribution function of one sample to another sample. Comparing the two distribution functions generates a D value, which represents the maximum distance between two curves, as well as a corresponding p-value.

Table A1: Repeat Sales Regression Results for Properties Sold Exactly Twice

	Dependent Variable: Log(Sales Price)						
	CRI_{365}	FD	SI	$REC_{>90}$	$REC_{>99}$	$DEC_{<10}$	$DEC_{<1}$
Index	-0.016***	-0.056***	-0.016	-0.002***	-0.006***	0.000	-0.002
	(0.005)	(0.021)	(0.015)	(0.000)	(0.002)	(0.000)	(0.002)
Index × Fire Risk	0.013***	0.069***	0.045***	0.002***	0.009***	-0.001	-0.007*
	(0.004)	(0.018)	(0.015)	(0.000)	(0.002)	(0.000)	(0.004)
Fire Risk × Year	-0.004**	-0.003*	-0.004**	-0.003**	-0.003*	-0.003**	-0.003**
	(0.002)	(0.002)	(0.002)	(0.002)	(0.002)	(0.002)	(0.002)
Num. Obs.	85,088	85,088	85,088	85,088	85,088	85,088	85,088
R^2	0.906	0.906	0.906	0.906	0.906	0.906	0.906
Adj. R^2	0.811	0.811	0.811	0.811	0.811	0.810	0.810
Property FE	Y	Y	Y	Y	Y	Y	Y
Year-month FE	Y	Y	Y	Y	Y	Y	Y
Census Time Trend	Y	Y	Y	Y	Y	Y	Y

Note: Significance levels: *** p<0.01, ** p<0.05, * p<0.1. Two-way clustered standard errors in parentheses. This table presents repeat sales regression results corresponding to Equation 9 for properties that only transacted twice. CRI_{365} (Cumulative Rainfall Index, 365-day), FD (Fractional Deviation), SI (Shock Index), REC (Rain Event Count), and DEC (Dry Event Count) are different measures of precipitation patterns. Subscripts for REC and DEC indicate percentile thresholds, with both measures calculated based on a 365-day lookback period.

Table A2: Repeat Sales Regression Results Excluding Speculative Transactions

	Dependent Variable: Log(Sales Price)						
	CRI_{365}	FD	SI	$REC_{>90}$	$REC_{>99}$	$DEC_{<10}$	$DEC_{<1}$
Index	-0.019***	-0.062**	-0.020	-0.003***	-0.008***	0.000	-0.006**
	(0.005)	(0.025)	(0.017)	(0.001)	(0.002)	(0.000)	(0.003)
Index × Fire Risk	0.017***	0.071***	0.047***	0.002***	0.013***	-0.001	-0.005
	(0.005)	(0.020)	(0.016)	(0.001)	(0.002)	(0.001)	(0.004)
Fire Risk × Year	-0.004***	-0.004**	-0.004***	-0.004***	-0.004**	-0.004***	-0.004***
	(0.002)	(0.002)	(0.002)	(0.002)	(0.002)	(0.002)	(0.002)
Num. Obs.	58,983	58,983	58,983	58,983	58,983	58,983	58,983
R^2	0.902	0.902	0.902	0.902	0.902	0.902	0.902
Adj. R^2	0.813	0.813	0.813	0.813	0.814	0.813	0.813
Property FE	Y	Y	Y	Y	Y	Y	Y
Year-month FE	Y	Y	Y	Y	Y	Y	Y
Census Time Trend	Y	Y	Y	Y	Y	Y	Y

Note: Significance levels: *** p<0.01, ** p<0.05, * p<0.1. Two-way clustered standard errors in parentheses. This table presents repeat sales regression results corresponding to Equation 9, excluding properties with holding periods less than four years. CRI_{365} (Cumulative Rainfall Index, 365-day), FD (Fractional Deviation), SI (Shock Index), REC (Rain Event Count), and DEC (Dry Event Count) are different measures of precipitation patterns. Subscripts for REC and DEC indicate percentile thresholds, with both measures calculated based on a 365-day lookback period.

narrative (Tables A1 and A2).

A.2 Salience

Figure A2 shows that public search interest in the terms "Windward" and "Leeward" has remained persistently high over time, comparable to that of "Condo," suggesting that microclimatic distinctions are widely recognized and salient in the context of Hawai'i's real estate market. Figure A3 complements this evidence by presenting sample Zillow listings in which sellers explicitly reference "Windward" or "Leeward" in property descriptions, indicating that these climatic terms are actively used to market homes. The consistent presence of such language in both search behavior and listings suggests that buyers are aware of, and respond to, Hawai'i's localized climatic variation.

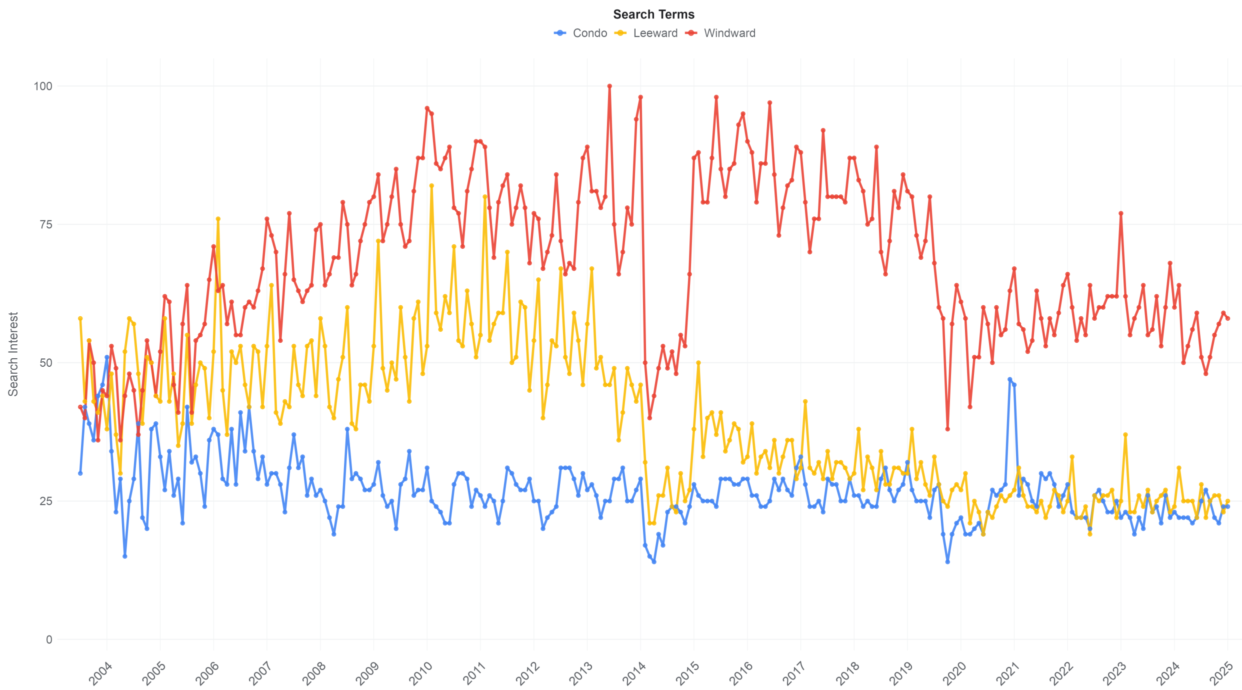

Figure A2: Google Trend Search Interest: Condo, Windward, Leeward

Note: This figure shows Google Trends search interest for three Hawai'i -related terms over time: Condo, Windward, and Leeward. Numbers represent search interest relative to the highest point on the chart for the given region and time. A value of 100 is the peak popularity for the term. A value of 50 means that the term is half as popular. A score of 0 indicates that there was insufficient data for this term.

A.3 Within Census Tract Variation and Spatial Correlation

To assess the plausibility of our identification strategy, we plot transaction-level cumulative rainfall exposure (CRI_{365}) within the census tract with the most sales for some selected years. We observe meaningful within-tract heterogeneity in precipitation exposure. These maps demonstrate that buyers within the same tract may face materially different climatic conditions, supporting our use of census tract-level fixed effects.

While our identification leverages within census tract variation, spatial correlation in rainfall, particularly among nearby properties, may be of concern (see Figure A4). To address this, we report standard errors corrected for spatial dependence using the Conley (1999) estimator. Similar to clustered standard errors which consider observations to not be independent of each other within groups, Conley standard errors allow for arbitrary correlation in the error structure among observations in close geographic proximity. We report results using a 2 km Haversine distance spatial cutoff. Our key findings remain robust to this correction and alternative cutoff definitions (up to 20 km).

What's special

Experience unparalleled stunning views of Kaneohe Bay & the Ko'olau mountains as you enter into this gated Hilltop Sanctuary! This 5 bedroom, 5/2 bathroom custom home sits atop the unique Windward neighborhood of Mahinui on Oahu— a hidden gem low-traffic area, just minutes from Kailua town & its beaches — boasting dynamic panoramic views of vibrant Kaneohe Bay, Kaneohe Yacht Club, Chinaman's Hat, and iconic Coconut Island.

Savor the ambience created by high ceilings, expansive rooms with large view windows, & an abundance of natural light.

Solidly built with all steel beam construction, hardwood flooring, travertine, imperial plaster walls, split AC; designed for everyday living and entertaining with two primary suites, large game room and bonus room, 3 entrances & separate living areas for extended family, friends or rental. Outdoor lounge and sundeck plus private back yard beckon you to relax or unwind & savor the fresh air of hilltop ocean breezes.

Proximity to H-3 on ramps allows you to live on the desirable lush Windward side, while still providing easy access to Honolulu and the airport.

What's special

Windward Wanderers wanted! Imagine moving to greener pastures with world famous Hoomaluhia Botanical Gardens nearby, hiking trails, shopping, restaurants, military base, Kaneohe Bay and more. Side by side washer dryer and cozy kitchen, make this home a must in your portfolio or even as your home. Pet friendly policies seem to attract the furriest of tenants, make sure to check the house rules. Take advantage of your Hawai'i Life by enjoying the natural beauty Oahu and the Windward side have to offer. Make it your own. Call today for a showing.

What's special

Makaha Surfside is a charming oceanfront community on Oahu's Leeward Coast, minutes from stunning beaches and scenic hiking trails. This move-in ready unit is a great opportunity for first-time homebuyers, investors, or if you're looking for a weekend retreat. Enjoy modern coastal living with a well-equipped kitchen featuring stainless steel appliances, an abundance of cabinet space plus the convenience of an in-unit washer and dryer. Resort-style amenities include two pools, beach access, surfboard storage, an exercise room, sauna, barbecue area and a 24-hr gated security. There is one assigned parking and also ample guest parking available. Don't miss your chance to own a piece of paradise - schedule a showing today!

What's special

OCEAN VIEW **CORNER UNIT** **VIBRANT TROPICAL PLANTS** **PALM TREES** **BRIGHT OPEN KITCHEN** **OPEN-CONCEPT LIVING** **TRANQUIL MOUNTAIN VIEWS**

Discover island living at Makaha Valley Plantation in this charming 2-bedroom, 1-bath corner unit nestled in the serene Leeward Coast. Tucked away in a peaceful we corner of the gated Makaha Valley Plantation community, this charming 2-bedroom, 1-bathroom condo has been recently updated with stylish vinyl floorin. Enjoy a bright open kitchen with a slight ocean view. This second-floor condo offers comfortable living space and tranquil mountain views. The gated community features resort-style amenities including a pool, sauna, and tennis courts—perfect for relaxation and recreation. Enjoy open-concept living and an open porch ideal for morning coffee or evening breezes. This unit represents strong value and ownership potential in one of Oahu's most scenic valleys. Ideal for first-time buyers, investors, or anyone seeking a peaceful Hawaii lifestyle. Includes two swimming pools, super convenient laundry facilities, plenty of guest parking, BBQ areas and courts for tennis and basketball. Vibrant tropical plants, lots of palm trees, and beautifully manicured lawns, all set against the stunning backdrop of the Waianae Mountain Range.

Figure A3: Sample Real Estate Listings

Note: This figure presents sample property listings from Zillow that explicitly reference Windward or Leeward in their descriptions, highlighting the salience of microclimatic terminology in Hawai'i's real estate market.

Figure A4: Within Census Tract Variation in CRI

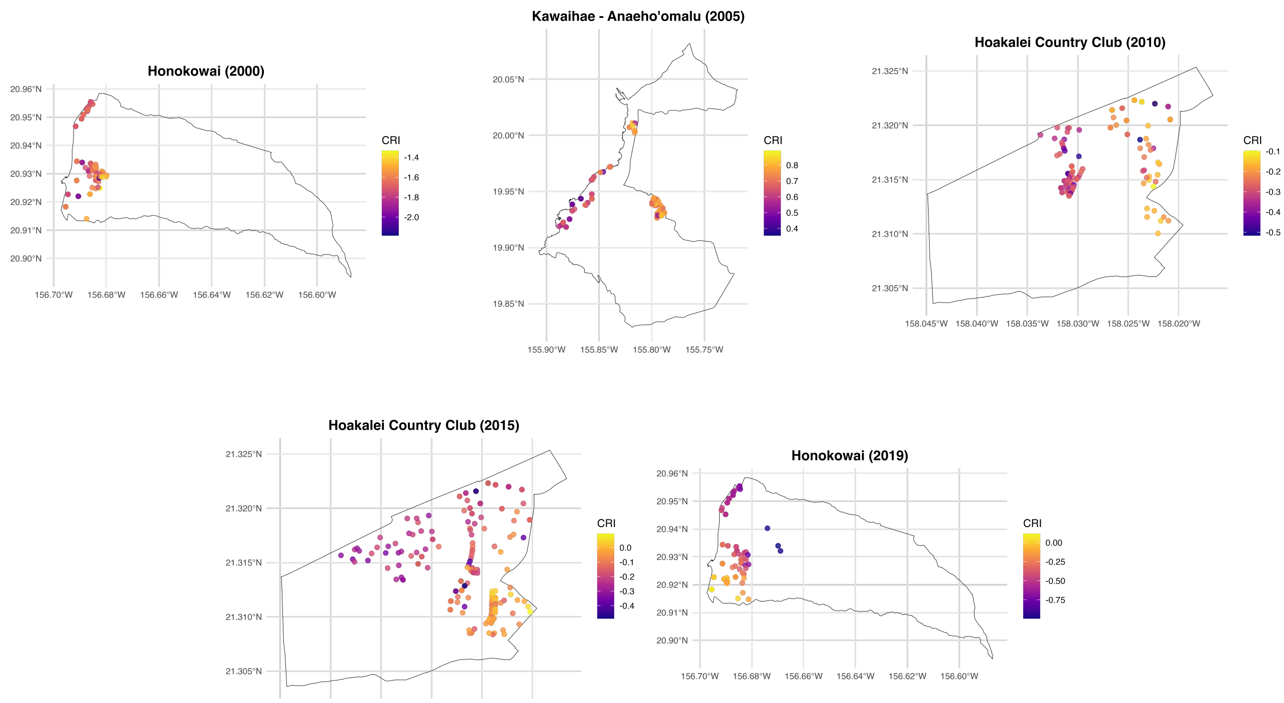

Note: This figure shows cumulative rainfall exposure (CRI_{365}) for transactions within the tract with the most sales across different years. We observe substantial within-tract variation in CRI.

Table A3: Hedonic Regression Results with Conley Standard Errors

	Dependent Variable: Log(Sales Price)						
	CRI_{365}	FD	SI	$REC_{>90}$	$REC_{>99}$	$DEC_{<10}$	$DEC_{<1}$
Index	-0.019***	-0.061***	-0.024	-0.003***	-0.008***	0.000	-0.005**
	(0.004)	(0.023)	(0.018)	(0.000)	(0.002)	(0.000)	(0.003)
Index × Fire Risk	0.011**	0.067***	0.042*	0.002***	0.010***	-0.001*	0.000
	(0.005)	(0.026)	(0.022)	(0.001)	(0.003)	(0.000)	(0.004)
Fire Risk	-0.083*	-0.086*	-0.084*	-0.148***	-0.124***	-0.061	-0.082*
	(0.047)	(0.047)	(0.047)	(0.051)	(0.048)	(0.051)	(0.047)
House Age	-0.004***	-0.004***	-0.004***	-0.004***	-0.004***	-0.004***	-0.004***
	(0.001)	(0.001)	(0.001)	(0.001)	(0.001)	(0.001)	(0.001)
Living Area (1000 sq. ft.)	0.252***	0.252***	0.252***	0.252***	0.252***	0.252***	0.252***
	(0.010)	(0.010)	(0.010)	(0.010)	(0.010)	(0.010)	(0.010)
Bedrooms	0.030***	0.030***	0.030***	0.030***	0.030***	0.030***	0.030***
	(0.009)	(0.009)	(0.009)	(0.009)	(0.009)	(0.009)	(0.009)
SFR	0.202***	0.201***	0.202***	0.202***	0.201***	0.202***	0.202***
	(0.015)	(0.015)	(0.015)	(0.015)	(0.015)	(0.015)	(0.015)
Avg. Slope	0.005***	0.005***	0.005***	0.005***	0.005***	0.005***	0.005***
	(0.002)	(0.002)	(0.002)	(0.002)	(0.002)	(0.002)	(0.002)
Num. Obs.	268,406	268,406	268,406	268,406	268,406	268,406	268,406
R^2	0.728	0.728	0.728	0.728	0.728	0.728	0.728
Adj. R^2	0.716	0.716	0.716	0.716	0.716	0.716	0.716
Census FE	Y	Y	Y	Y	Y	Y	Y
Year-month FE	Y	Y	Y	Y	Y	Y	Y
Conley SE	2km	2km	2km	2km	2km	2km	2km

Note: Significance levels: *** p<0.01, ** p<0.05, * p<0.1. This table presents hedonic regression results corresponding to Equation 8. CRI_{365} (Cumulative Rainfall Index, 365-day), FD (Fractional Deviation), SI (Shock Index), REC (Rain Event Count), and DEC (Dry Event Count) are different measures of precipitation patterns. Subscripts for REC and DEC indicate percentile thresholds, with both measures calculated based on a 365-day lookback period. All models include twenty equal sized control bins for elevation and coastal proximity. We use Conley standard errors to recognize potential dependence of observations based on spatial proximity (2km cutoff).

A.4 Dynamic Fire Risk

Our fire risk designation is based on wildfire risk zones established in the mid-2000s, with boundaries remaining constant from data collection in 2006-2007 to the end of our sample period in 2019. While research shows that home buyers respond to such risk designations (Donovan et al., 2007), Figure A5 reveals that actual wildfire occurrences do not perfectly align with these established risk zones. Another concern is that wildfire risk tends to be capitalized into housing prices only in the aftermath of salient events, such as nearby fires, and these effects typically dissipate within a few years (Bin and Landry, 2013; McCoy and Walsh, 2018). To validate our findings, we construct a time-varying fire exposure index based on actual wildfire occurrences within three years of each transaction.

We obtain the wildfire occurrence data from the Pacific Fire Exchange website. The dataset primarily focuses on fires equal to or larger than 20 hectares (50 acres) and integrates multiple data sources including ground-based GPS-mapped fire perimeters from the Hawai'i Wildfire Management Organization, National Park Service records from Hawai'i Volcanoes

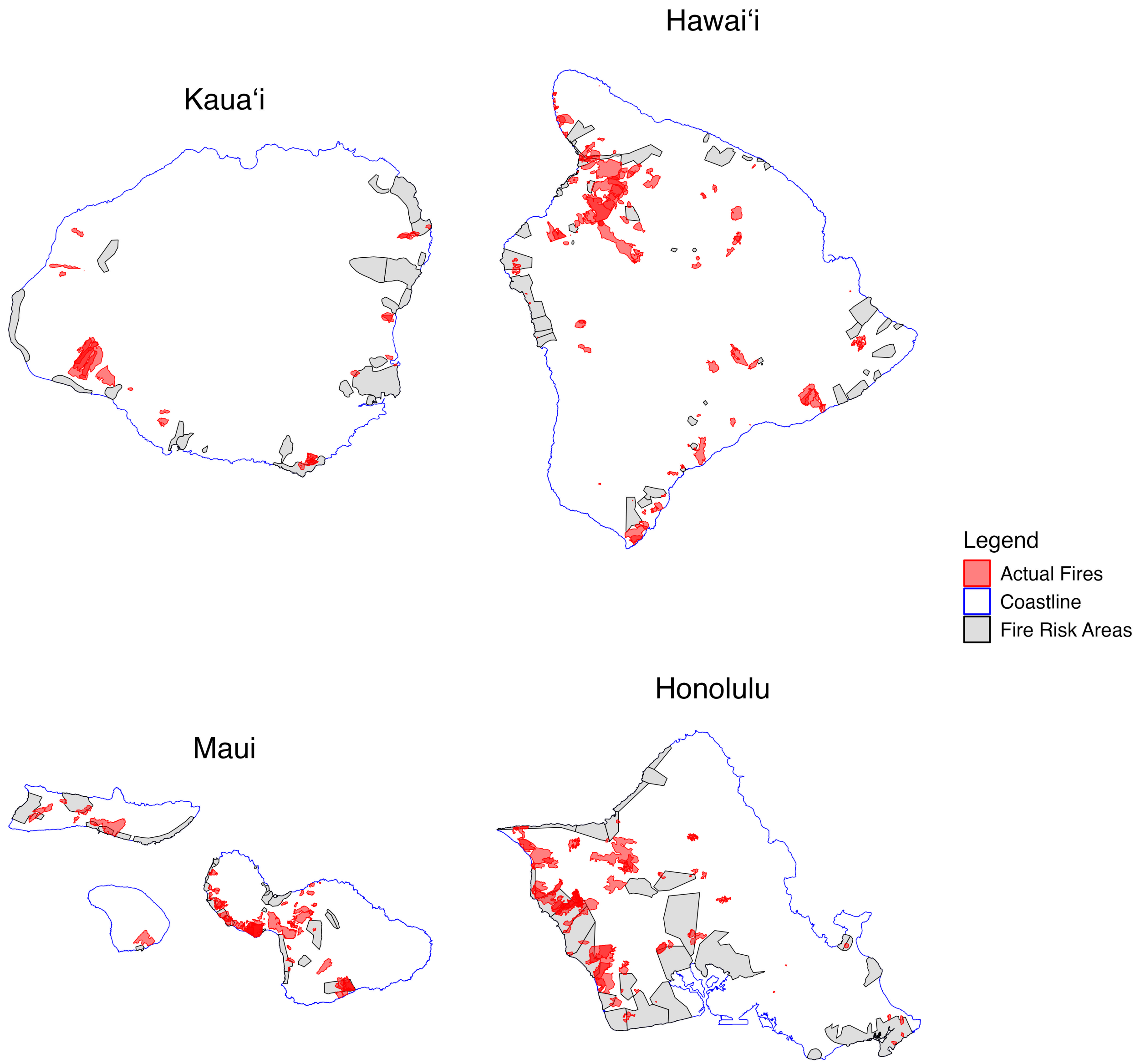

Figure A5: Actual Fire Occurrences and Fire Risk Areas

National Park, US Geological Survey's Monitoring Trends in Burn Severity satellite data (2002-2011), and the Army Natural Resource Program-Oahu. Additional fires were mapped by the University of Hawaiʻi's Department of Natural Resources and Environmental Management using LANDSAT and Sentinel-2 satellite imagery. The state had a total of 310 wildfires between 2000-2019, with an average size of 796 acres.

Existing literature typically employs either the size and proximity of the nearest fire (Holmes et al., 2008; Stetler et al., 2010) or considers the number and average size of fires within a set distance from properties (Hansen and Naughton, 2013; Xu and Van Kooten, 2013), finding significant impacts on property values. However, using these attributes individually can overlook the non-linear relationships between fire exposure and property values, potentially missing relevant fire characteristics. To circumvent these issues, we construct a transaction-specific index following Shi et al. (2022). This measure integrates all major aspects of wildfire exposure; fire sizes, distances to fires, and the number of fires. Specifically, for each property transaction i at time t, we calculate:

$$\text{FireIndex}_{it} = \sum_k \frac{\text{size}_{kt}^{\alpha}}{\exp(\text{distance}_{kt})} \tag{10}$$

where size_{kt} represents the size of fire k in acres, distance_{kt} indicates the proximity in km from the property to the centroid of fire k, and α is a diminishing parameter. This measure allows for nonlinear impacts of fire size while accounting for spatial decay in the fire's influence through the exponential distance term, and is also similar to indices used in other papers assessing the impact of environmental hazards on property values (see, for example, McCluskey and Rausser, 2001; Ready and Abdalla, 2005; Gopalakrishnan and Klaiber, 2014).

Following Shi et al. (2022), we use wildfires occurring between three years and 60 days before the sale date to construct the fire index. The lower limit of 60 days is selected because the decision to purchase a property is often made around two months before the official recording date, as commonly noted in hedonic studies (Loomis, 2004; Mueller et al., 2009). The upper limit of three years is informed by literature indicating that initial high price discounts due to wildfire risk tend to diminish over a 2–3-year period (McCoy and Walsh, 2018). We further restrict our analysis to wildfires within 10 km of the property.[6] Prior studies indicate that wildfires beyond 20 km generally do not significantly affect property values (Stetler, 2008; Stetler et al., 2010), which has led to 20 km being a standard search radius in previous research (Shi et al., 2022). However, we adopt a 10 km radius, as the geographic area in our study is generally smaller than those examined in these earlier works.

We employ the conventional grid search method, which exhaustively searches through a manually specified subset of possible values for α (Dufour and Neves, 2019; Shi et al., 2022). Specifically, for each candidate value of α between $[-2, 2]$ in increments of 0.1, we calculate the fire index and estimate our hedonic model separately, selecting the value that minimizes the sum of squared residuals (SSR). To quantify uncertainty around our optimal estimate, we perform 100 bootstrap replications, randomly resampling our data with replacement, and re-running the entire grid search procedure for each sample to calculate standard errors and confidence intervals for α. Our estimated optimal α of 0.2 falls well within the uncertainty interval derived from this bootstrap procedure and remains consistent across all hedonic model specifications with different rainfall measures. Previous studies suggest that α should be relatively small, likely within the range of 0 to 1, indicating a diminishing marginal impact of fire size on property values (Xu and Van Kooten, 2013; Shi et al., 2022). In this context, our estimate of $\alpha = 0.2$ aligns well with existing literature and represents a statistically reliable estimate of the diminishing marginal impact of fire size on property values.

Table A4 presents summary statistics for the newly added fire-related variables, using the same sample as the previously analyzed dataset. Overall, 43% of transactions in the sample had some level of wildfire exposure. The mean fire index value of 0.41 and median of 0 suggest that most of these properties had low fire exposure. The maximum fire index value of 18 highlights that certain properties were situated in significantly high-risk zones.

Pearson correlations among key variables assess the extent of dependence between our fire risk and precipitation measures (Figure A6). The fire risk zone indicator correlates positively with our dynamic fire exposure index, suggesting

[6] We calculate distances from the center of each property to the centroid of each fire polygon, reflecting the assumption that a fire's impact emanates from its center.

Table A4: Summary Statistics for Fire Index Sample (2000-2019)

	Mean	Median	Sd	Min.	Max.
Fire Index	0.41	0	1.1	0	18
Fire Index > 0	0.43	0	0.5	0	1

Note: Descriptive statistics for the fire index sample for the four islands of Maui, Kaua'i , Honolulu, and Hawai'i . The variable "Fire Index > 0" is a dummy, equal to 1 if the fire index for a transaction is positive. N = 268,406.

consistency between designated risk areas and actual fire patterns. Precipitation measures exhibit expected correlations with each other but show minimal correlation with either fire risk measure, supporting the identification of interaction effects in our main analysis.

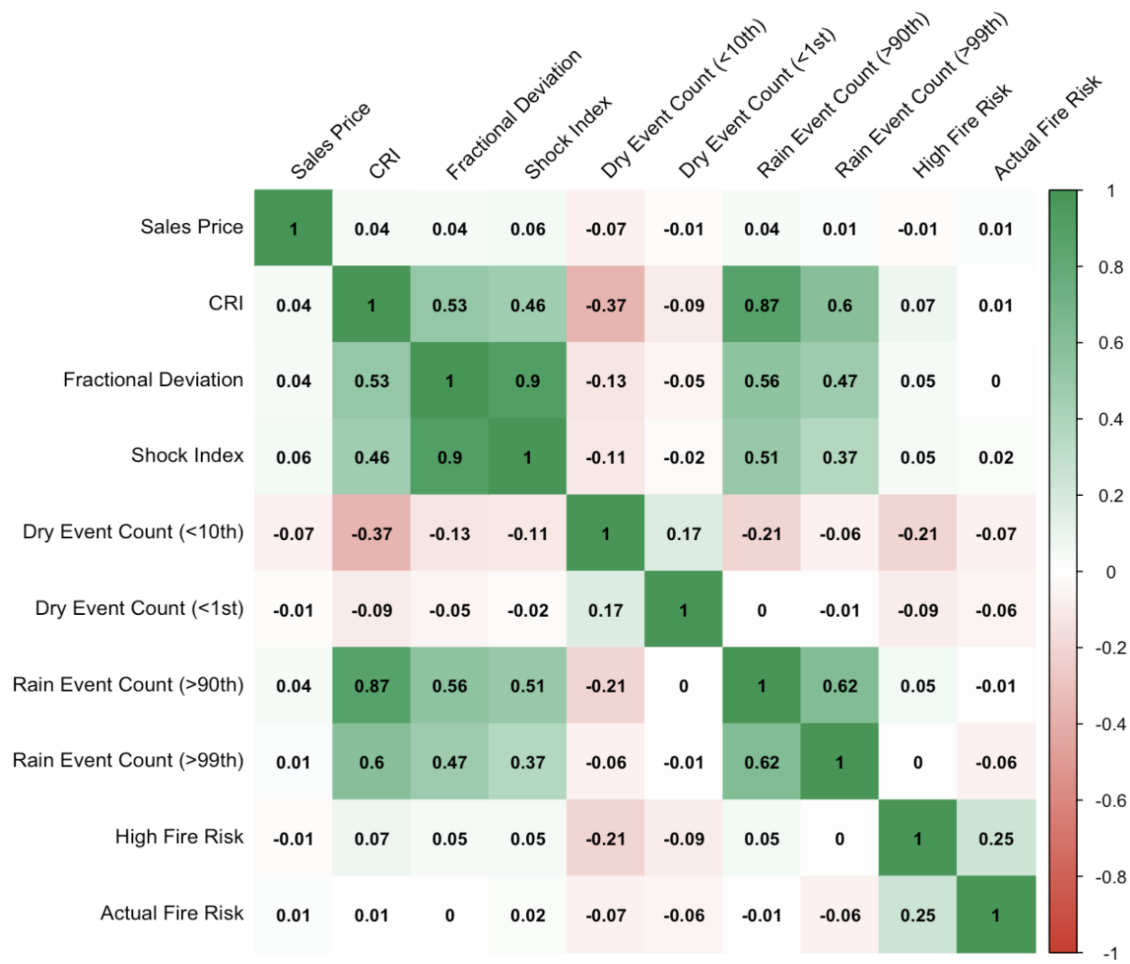

Figure A6: Correlation Matrix

Note: Lookback period is 365 days where applicable.

We now estimate our main hedonic specification using the time-varying fire index measure as opposed to the fire risk designation. Table A5 reinforces our core findings while providing additional robustness. The results continue to demonstrate the dual negative effects of both rainfall and wildfire risk on property values. More importantly, they substantiate our primary hypothesis regarding rainfall's moderating effect on wildfire risk. Specifically, in areas considered safe from fires, a one unit higher CRI, representing one standard deviation higher rainfall at a particular location, corresponds to 1.5% lower property values. However, for properties in fire-prone areas that experienced rainfall, this negative effect is reduced to approximately 1%. This pattern, observed across both static and dynamic measures of fire risk, provides robust evidence for our central finding: rainfall significantly mitigates the negative impact of being in a fire-prone area. We also find some support ($p < 0.1$) that each additional dry day further reduces property values in areas at risk of wildfire.

Table A5: Hedonic Regression Results with Fire Index

	Dependent Variable: Log(Sales Price)						
	CRI_{365}	FD	SI	$REC_{>90}$	$REC_{>99}$	$DEC_{<10}$	$DEC_{<1}$
Index	-0.015***	-0.019**	-0.001	-0.002***	-0.003*	-0.001***	-0.006***
	(0.003)	(0.011)	(0.009)	(0.000)	(0.001)	(0.000)	(0.001)
Fire Index	-0.011***	-0.011***	-0.011***	-0.034***	-0.021***	-0.022***	-0.011***
	(0.003)	(0.003)	(0.003)	(0.005)	(0.004)	(0.004)	(0.003)
Index × Fire Index	0.006***	0.018***	0.013***	0.001***	0.003***	-0.001***	-0.003*
	(0.001)	(0.004)	(0.003)	(0.000)	(0.001)	(0.000)	(0.002)
House Age	-0.004***	-0.004***	-0.004***	-0.004***	-0.004***	-0.004***	-0.004***
	(0.000)	(0.000)	(0.000)	(0.000)	(0.000)	(0.000)	(0.000)
Living Area (1000 sq. ft.)	0.252***	0.252***	0.252***	0.252***	0.252***	0.252***	0.252***
	(0.006)	(0.006)	(0.006)	(0.006)	(0.006)	(0.006)	(0.006)
Bedrooms	0.030***	0.030***	0.030***	0.030***	0.030***	0.030***	0.030***
	(0.003)	(0.003)	(0.003)	(0.003)	(0.003)	(0.003)	(0.003)
SFR	0.202***	0.202***	0.202***	0.202***	0.202***	0.202***	0.202***
	(0.009)	(0.009)	(0.009)	(0.009)	(0.009)	(0.009)	(0.009)
Avg. Slope	0.005***	0.005***	0.005***	0.005***	0.005***	0.005***	0.005***
	(0.001)	(0.001)	(0.001)	(0.001)	(0.001)	(0.001)	(0.001)
Num. Obs.	268,406	268,406	268,406	268,406	268,406	268,406	268,406
R^2	0.728	0.728	0.728	0.728	0.728	0.728	0.728
Adj. R^2	0.716	0.716	0.716	0.716	0.716	0.716	0.716
Census FE	Y	Y	Y	Y	Y	Y	Y
Year-month FE	Y	Y	Y	Y	Y	Y	Y

Note: Significance levels: *** p<0.01, ** p<0.05, * p<0.1. Two-way clustered standard errors in parentheses. This table presents hedonic regression results corresponding to Equation 8 but using the dynamic fire risk measure. CRI_{365} (Cumulative Rainfall Index, 365-day), FD (Fractional Deviation), SI (Shock Index), REC (Rain Event Count), and DEC (Dry Event Count) are different measures of precipitation patterns. Subscripts for REC and DEC indicate percentile thresholds, with both measures calculated based on a 365-day lookback period. All models include twenty equal sized control bins for elevation and coastal proximity.

A.5 Precipitation Measures

We show that our results are not sensitive to the choice of lookback period before the property transaction. We consider the alternative construction of the cumulative rainfall index with lookbacks of 90 and 180 days respectively. We also consider the impact of Rain and Dry Event counts based on various percentile thresholds. Table A6, A7, and A8 report these results.

The Cumulative Rain Index (CRI) captures broad precipitation patterns over 90, 180, and 365 day lookbacks, comparing them to either fixed historical (1990-1999) or dynamic (prior decade) baselines. Table A9 reports fixed baseline results.

Table A6: Hedonic Regression Results with Different Lookbacks for CRI

	Dependent Variable: Log(Sales Price)			
Lookback Days	180	90	180	90
CRI	-0.015***	-0.010***	-0.010***	-0.007**
	(0.004)	(0.004)	(0.003)	(0.003)
Fire Risk	-0.084**	-0.083**		
	(0.038)	(0.038)		
CRI × Fire Risk	0.010***	0.007***		
	(0.002)	(0.003)		
Fire Index			-0.011***	-0.011***
			(0.003)	(0.003)
CRI × Fire Index			0.005***	0.003***
			(0.001)	(0.001)
House Age	-0.004***	-0.004***	-0.004***	-0.004***
	(0.000)	(0.000)	(0.000)	(0.000)
Living Area (1000 sq. ft.)	0.252***	0.252***	0.252***	0.252***
	(0.006)	(0.006)	(0.006)	(0.006)
Bedrooms	0.030***	0.030***	0.030***	0.030***
	(0.003)	(0.003)	(0.003)	(0.003)
SFR	0.201***	0.201***	0.200***	0.200***
	(0.009)	(0.009)	(0.009)	(0.009)
Avg. Slope	0.005***	0.005***	0.005***	0.005***
	(0.001)	(0.001)	(0.001)	(0.001)
Num. Obs.	268,406	268,406	268,406	268,406
R^2	0.728	0.728	0.728	0.728
Adj. R^2	0.716	0.716	0.716	0.716
Census FE	Y	Y	Y	Y
Year-month FE	Y	Y	Y	Y

Note: Significance levels: *** p<0.01, ** p<0.05, * p<0.1. Two-way clustered standard errors are in parentheses. This table presents hedonic regression results corresponding to Equation 8 using different lookback periods for the Cumulative Rainfall Index. It incorporates both static and dynamic fire risk measures.

Both CRI and Fire Risk coefficients maintain similar magnitudes and statistical significance across specifications.[7] However, the positive interaction between rainfall index and fire risk, is only significant in one of three models under fixed baseline. Overall, the similarities between rolling and fixed baseline patterns are not distinct enough to suggest that buyers perceive recent rainfall as less impactful in the longer run having had more time to adjust to the climate norm.

[7]Under the fixed baseline specification, the CRI coefficients were consistently negative: -1.9% (365-day), -1.5% (180-day), and -1.0% (90-day), with all coefficients significant at 1% level. In dynamic baseline, these are -1.7%, -1.1%, and -0.7%, respectively, significant at either 1% or 5% level. In both cases, Fire Risk coefficient is approximately -0.8%, significant at 5% level (see Tables 4 & A6).

Table A7: Hedonic Regression Results with Different Lookbacks for REC

	Dependent Variable: Log(Sales Price)						
	365 Days	180 Days			90 Days		
	$REC_{>95}$	$REC_{>99}$	$REC_{>95}$	$REC_{>90}$	$REC_{>99}$	$REC_{>95}$	$REC_{>90}$
Index	-0.005***	-0.006***	-0.004***	-0.003***	-0.002	-0.004***	-0.003***
	(0.001)	(0.002)	(0.001)	(0.000)	(0.002)	(0.001)	(0.001)
Index × Fire Risk	0.003***	0.010***	0.003***	0.002***	0.009***	0.003***	0.002***
	(0.000)	(0.001)	(0.001)	(0.000)	(0.002)	(0.001)	(0.001)
Fire Risk	-0.147***	-0.106***	-0.113***	-0.112***	-0.093**	-0.098**	-0.099***
	(0.039)	(0.038)	(0.038)	(0.038)	(0.038)	(0.038)	(0.038)
House Age	-0.004***	-0.004***	-0.004***	-0.004***	-0.004***	-0.004***	-0.004***
	(0.000)	(0.000)	(0.000)	(0.000)	(0.000)	(0.000)	(0.000)
Living Area (1000 sq. ft.)	0.252***	0.252***	0.252***	0.252***	0.252***	0.252***	0.252***
	(0.006)	(0.006)	(0.006)	(0.006)	(0.006)	(0.006)	(0.006)
Bedrooms	0.030***	0.030***	0.030***	0.030***	0.030***	0.030***	0.030***
	(0.003)	(0.003)	(0.003)	(0.003)	(0.003)	(0.003)	(0.003)
SFR	0.202***	0.201***	0.201***	0.202***	0.201***	0.201***	0.202***
	(0.009)	(0.009)	(0.009)	(0.009)	(0.009)	(0.009)	(0.009)
Avg. Slope	0.005***	0.005***	0.005***	0.005***	0.005***	0.005***	0.005***
	(0.001)	(0.001)	(0.001)	(0.001)	(0.001)	(0.001)	(0.001)
Num. Obs.	268,406	268,406	268,406	268,406	268,406	268,406	268,406
R^2	0.729	0.728	0.728	0.728	0.728	0.728	0.728
Adj. R^2	0.716	0.716	0.716	0.716	0.716	0.716	0.716
Census FE	Y	Y	Y	Y	Y	Y	Y
Year-month FE	Y	Y	Y	Y	Y	Y	Y

Note: Significance levels: *** p<0.01, ** p<0.05, * p<0.1. Two-way clustered standard errors in parentheses. This table presents hedonic regression results corresponding to Equation 8. REC (Rain Event Count) variables are partitioned by lookback periods (365, 180, 90 days) and percentile thresholds (99, 95, 90).

Table A8: Hedonic Regression Results with Different Lookbacks for DEC

	Dependent Variable: Log(Sales Price)						
	365 Days	180 Days			90 Days		
	$DEC_{<5}$	$DEC_{<10}$	$DEC_{<5}$	$DEC_{<1}$	$DEC_{<10}$	$DEC_{<5}$	$DEC_{<1}$
Index	-0.001*	0.000	0.000	-0.004**	0.001	0.000	-0.006**
	(0.000)	(0.000)	(0.001)	(0.002)	(0.001)	(0.001)	(0.002)
Index × Fire Risk	0.000	-0.001*	-0.001	0.001	0.000	0.000	0.004
	(0.000)	(0.000)	(0.001)	(0.003)	(0.001)	(0.001)	(0.003)
Fire Risk	-0.080**	-0.073**	-0.078**	-0.083**	-0.081**	-0.083**	-0.083**
	(0.039)	(0.038)	(0.038)	(0.038)	(0.039)	(0.038)	(0.038)
House Age	-0.004***	-0.004***	-0.004***	-0.004***	-0.004***	-0.004***	-0.004***
	(0.000)	(0.000)	(0.000)	(0.000)	(0.000)	(0.000)	(0.000)
Living Area (1000 sq. ft.)	0.252***	0.252***	0.252***	0.252***	0.252***	0.252***	0.252***
	(0.006)	(0.006)	(0.006)	(0.006)	(0.006)	(0.006)	(0.006)
Bedrooms	0.030***	0.030***	0.030***	0.030***	0.030***	0.030***	0.030***
	(0.003)	(0.003)	(0.003)	(0.003)	(0.003)	(0.003)	(0.003)
SFR	0.202***	0.202***	0.202***	0.202***	0.202***	0.202***	0.202***
	(0.009)	(0.009)	(0.009)	(0.009)	(0.009)	(0.009)	(0.009)
Avg. Slope	0.005***	0.005***	0.005***	0.005***	0.005***	0.005***	0.005***
	(0.001)	(0.001)	(0.001)	(0.001)	(0.001)	(0.001)	(0.001)
Num. Obs.	268,406	268,406	268,406	268,406	268,406	268,406	268,406
R^2	0.728	0.728	0.728	0.728	0.728	0.728	0.728
Adj. R^2	0.716	0.716	0.716	0.716	0.716	0.716	0.716
Census FE	Y	Y	Y	Y	Y	Y	Y
Year-month FE	Y	Y	Y	Y	Y	Y	Y

Note: Significance levels: *** p<0.01, ** p<0.05, * p<0.1. Two-way clustered standard errors in parentheses. This table presents hedonic regression results corresponding to Equation 8. DEC (Dry Event Count) variables are partitioned by lookback periods (365, 180, 90 days) and percentile thresholds (10, 5, 1).

Table A9: Hedonic Regression Results with Different Lookbacks for CRI (1990-1999 base)

	Dependent Variable: Log(Sales Price)		
Lookback Days	365	180	90
CRI	-0.017***	-0.011***	-0.007**
	(0.003)	(0.004)	(0.004)
Fire Risk	-0.080**	-0.082**	-0.082**
	(0.038)	(0.038)	(0.038)
CRI × Fire Risk	0.006**	0.004	0.002
	(0.003)	(0.003)	(0.003)
House Age	-0.004***	-0.004***	-0.004***
	(0.000)	(0.000)	(0.000)
Living Area (1000 sq. ft.)	0.252***	0.252***	0.252***
	(0.006)	(0.006)	(0.006)
Bedrooms	0.030***	0.030***	0.030***
	(0.003)	(0.003)	(0.003)
SFR	0.201***	0.201***	0.201***
	(0.009)	(0.009)	(0.009)
Avg. Slope	0.005***	0.005***	0.005***
	(0.001)	(0.001)	(0.001)
Num. Obs.	268,406	268,406	268,406
R^2	0.728	0.728	0.728
Adj. R^2	0.716	0.716	0.716
Census FE	Y	Y	Y
Year-month FE	Y	Y	Y

Note: Significance levels: *** $p<0.01$, ** $p<0.05$, * $p<0.1$. Two-way clustered standard errors are presented in parentheses. This table presents hedonic regression results corresponding to Equation 8 using different lookback periods (365, 180, and 90 days) for the Cumulative Rainfall Index, where each period's rainfall is compared to the same calendar days in the fixed base period of 1990-1999.